Polysaccharides enzymatic modification to control the coacervation or the aggregation behavior: a thermodynamic study

Marie E. Vuillemin, Florentin Michaux, Aurélie Seiler, Michel Linder, Lionel Muniglia, Jordane Jasniewski

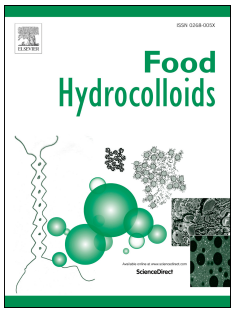

Polysaccharides enzymatic modification to control the coacervation or the aggregation behavior: a thermodynamic study

Marie E. Vuillemin, Florentin Michaux, Aurélie Seiler, Michel Linder, Lionel Muniglia, Jordane Jasniewski

PII: S0268-005X(21)00508-7

DOI: https://doi.org/10.1016/j.foodhyd.2021.107092

Reference: FOOHYD 107092

To appear in: *Food Hydrocolloids*

Received Date: 7 May 2021

Revised Date: 21 July 2021

Accepted Date: 4 August 2021

Please cite this article as: Vuillemin, M.E., Michaux, F., Seiler, A., Linder, M., Muniglia, L., Jasniewski, J., Polysaccharides enzymatic modification to control the coacervation or the aggregation behavior: a thermodynamic study, *Food Hydrocolloids*, https://doi.org/10.1016/j.foodhyd.2021.107092.

Marie E. Vuillemin Conceptualization; Formal analysis; Investigation; Data curation; Writing - original draft

Florentin Michaux Conceptualization ; Validation; Data curation; Supervision; Writing - review & editing

Aurélie Seiler Investigation; Data curation;

Michel Linder Writing - review & editing

Lionel Muniglia Writing - review & editing

Jordane Jasniewski Conceptualization; Methodology; Data curation; Validation; Supervision; Writing - review & editing

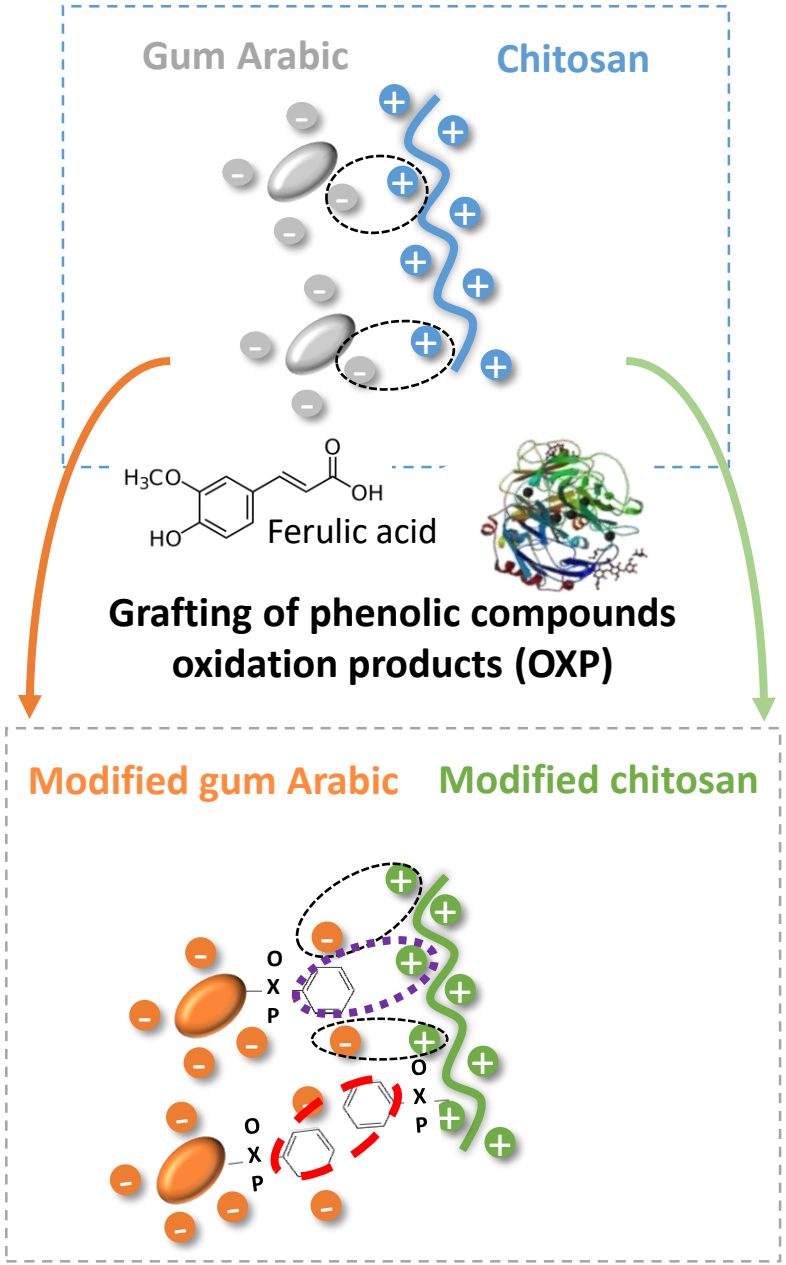

Coacervation

Electrostatic interactions

New interactions: Aggregation

Electrostatic interactions
π-cation interaction
π-π stacking

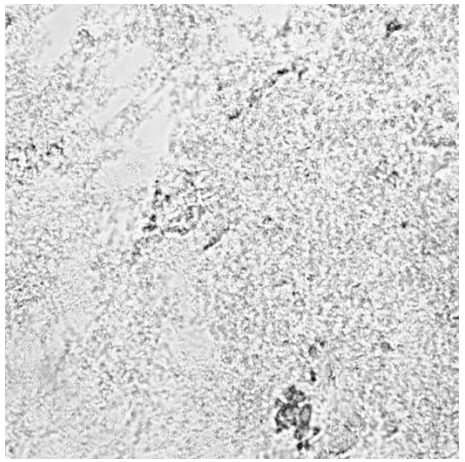

Polysaccharides enzymatic modification to control the coacervation or the aggregation behavior: a thermodynamic study

Marie E. Vuillemin, Florentin Michaux, Aurélie Seiler, Michel Linder, Lionel Muniglia and Jordane Jasniewski *

*Corresponding author: jordane.jasniewski@univ-lorraine.fr

Université de Lorraine, LIBio, F-54000 Nancy, France

Abstract

The effect of enzymatic modification of polysaccharides on the formed supramolecular structures was studied. Gum Arabic and chitosan were modified by covalent grafting of ferulic acid oxidation products so that they could establish new interactions such as π interactions. The stoichiometry of the interaction was studied by ITC measurements, as well as its strength and related thermodynamic parameters. These experiments were supported by Zeta potential and turbidity measurements and optical macroscopy observations. Grafting of phenolic compounds onto the polymers increased their ability to exhibit π-π stacking and π-cation interactions and led to the formation of various supramolecular structures. For native gum Arabic and chitosan assemblies, the stoichiometry value determined by ITC was consistent with optical microscopy, macroscopic observations and Zeta potential (around a molar ratio gum Arabic:chitosan of 3). The structures formed were coacervates. For the modified polymers, the optimal molar ratio determined by Zeta potential measurements (3.27) differed from the one determined by ITC (6.3). This meant the formation aggregates was not only due to electrostatic interactions but also to other type of interactions (new π-π stacking and π-cation interactions). It was concluded that by modifying the polymers, it was possible to control the supramolecular structures formed.

Keywords: Complex coacervation; supramolecular structures; Isothermal titration calorimetry; gum Arabic; chitosan; interactions.

1. Introduction

The balance of interactions between molecules or between molecules and solvent represents the driving force for the formation of self-assembled colloidal systems. In recent years, the compartmentalized environments of cells have been mimicked in bottom- up systems through the use of condensed polymeric phases (Aumiller et al., 2016; Crowe & Keating, 2018; Jia et al., 2014; Poudyal et al., 2019). In these phases, oppositely charged polyelectrolytes condense into a polymer- rich phase due to their mutual electrostatic interactions. This process is called complex coacervation (Yewdall et al., 2019). Coacervates result from spontaneous mechanisms coming from interactions between building blocks as surfactants, proteins, polysaccharides (Kötz et al., 2001; Meyer et al., 2006). Several types of interactions can exist to produce such complex structures as electrostatic, hydrophobic, Van der Waals (Sahoo et al., 2018; Whitesides et al., 1991). These are described by their strength and their range (Campbell & Reece, 2004; Neel et al., 2017).

The understanding of the formation of supramolecular structures represents a key point to consider a possible control of the organization at the colloidal scale. Modifying the interactions in a given system to investigate their influence on the colloidal structure formed is therefore of major interest. There are two ways of modifying these interactions. The first one consists in controlling the physical-chemical properties of the medium like pH and/or ionic strength to modify electrostatic interactions for example. This strategy is well known and widely reported in the literature (Butstraen & Salaün, 2014; Coelho et al., 2011; Espinosa-Andrews et al., 2007; Kizilay et al., 2011; Vuillemin et al., 2019). To modify interactions between two molecules, a

second possible strategy is to chemically modify the building blocks. This can lead to decrease, suppress or strengthen some potential interactions. Assemblies formed from biopolymers (protein, polysaccharides) appear to be good candidates for this purpose since the structures formed depend on the type and strength of the interaction. Since these molecules are often polyelectrolytes, electrostatic interactions frequently direct the formation of complexes, coacervates or aggregates. It is recognized that strong interactions between the building blocks mainly lead to the formation of aggregates while weaker interactions promote the formation of coacervates (Comert and Dubin, 2017). Modifying the chemical structures of the molecules can change their interactions and lead to controlling the resulting colloidal structure. In this work, the influence of chemical modifications of polysaccharides on the supramolecular structure they spontaneously form in an aqueous phase was investigated. Therefore, Gum Arabic (GA) and chitosan (CN) were chosen for their ability to interact *via* electrostatic interactions in a given pH range and spontaneously form coacervates in water (Vuillemin et al., 2019).

CN is a polymer of glucosamine and N-acetyl glucosamine linked by β (1–4) glycosidic bonds (Soni et al., 2018). It is derived from the deacetylation of chitin from crustacean shells. The free amino groups of chitosan are protonated in solution, when the pH is below its pKa (i.e. between 6.3 and 7.0 (Beppu & Santana, 2002)). In other words, CN is positively charged when protonated, which remains a property that few polysaccharides exhibit and it is the primary reason that led to the choice of CN in several studies on complex coacervation (Avadi et al., 2010; Butstraen & Salauen, 2014; Espinosa-Andrews et al., 2007, 2010; Maqbool et al., 2010; Roldan-Cruz et al., 2016; Sakloetsakun et al., 2015; Tan et al., 2016). Moreover, it has an extended conformation in acetic acid solution, so its charges are accessible (Espinosa-Andrews et al., 2007; Schatz et al., 2004). Furthermore, it possesses attractive properties as this biopolymer is film-forming, biodegradable, biocompatible and exhibits antimicrobial and antioxidant activities (Fathi et al., 2014; Soni et al., 2018; Sonia & Sharma, 2012).

CN was chosen as the polycation for this study and GA was selected as the polyanion. GA is a sticky exudate of air-solidified tree sap from the stems or branches of Acacia trees (Avadi et al., 2010). There are several species of Acacia. However, the two most exploited species are *Acacia senegal* and *Acacia seyal*, which essentially produce brittle gum (McNamee et al., 1998). GA contains three peculiar fractions: 85–90 wt. % of arabinogalactan, 10 wt. % of arabinogalactan-protein complex and 2 wt. % of one or two glycoproteins (Lopez-Torrez et al., 2015). These fractions confer several different chemical groups to gum Arabic. It possesses amino groups due to its protein content. In addition, it contains carboxyl groups present on its glucuronic acid residues (Padala et al., 2009), which are responsible for the charge of GA in aqueous solution above its pKa of 3.6. GA is a hydrophilic polysaccharide that is highly soluble in water. It has a globular structure in aqueous solution (Moschakis et al., 2010; Renard et al., 2012). Furthermore, it is used in various industrial applications as an additive in food formulation (E414) or for encapsulation (Mosquera et al., 2012), for vectorization in the pharmaceutical industry (Avadi et al., 2010; Bosnea et al., 2014, 2017), as an adhesive in the cosmetic industry and for various other applications (Verbeken et al., 2003).

Several authors have already studied the complex coacervation of GA and CN (Butstraen & Salaün, 2014; Coelho et al., 2011; Espinosa-Andrews et al., 2007, 2013; Tan et al., 2016). The influence of several parameters such as pH, ionic strength, temperature, or polyelectrolyte concentration on GA and CN coacervation has been well characterized but there is still a need to deepen the knowledge on the thermodynamic pathways that govern this phenomenon. In recent studies, the mechanism of coacervate formation and the thermodynamic parameters driving the complex formation have been investigated (Vuillemin et al., 2019). It was demonstrated that pH and temperature affected the thermodynamics of GA-CN interactions (especially at 45 °C and pH 5.5) and that coacervation was driven by enthalpy. The electrical charges arise from the presence of negatively charged carboxylic groups on GA and positively

charged amine groups on CN, respectively. These chemical groups can be easily modified to induce (i) a decrease in electrical charge by replacing the chemical function with another chemical group and (ii) an addition of new functional groups that can introduce new possible interactions, thus obtaining different supramolecular structures.

Some authors have previously attempted to modify chitosan by chemical methods to shed light on the impact of modification on coacervate formation with gum Arabic (Huang et al., 2015, 2016, 2017). They showed that modification of chitosan by N, O-carboxymethylation or O-carboxymethylation reduced electrostatic interactions while maintaining high coacervation yields. Other driving forces such as hydrophobic interaction could be considered for chitosan and gum Arabic to form coacervates, especially at high temperatures. This could initially lead to a deeper understanding of the mechanisms and forces driving complex formation. The modification of polymers could lead to different conditions of complex formation than the optimal ones obtained with native polymers and to the formation of different supramolecular structures (particles, aggregates, coacervates…). However, the modification route used in existing studies on the subject is chemical modification. To make this strategy green and to modify chitosan and gum Arabic using the same methodology, a sustainable way consists in an approach using the laccase-catalyzed oxidation reaction of ferulic acid. This approach has the advantage of being eco-acceptable, as it is implemented under mild, aqueous conditions and at room temperature. Besides, it is not extremely specific and can be implemented on a considerable number of substrates. However, this method presents some disadvantages, such as the fact that the reaction is difficult to control, the products can be grafted at various locations, and the structure of the products formed remains poorly understood. However, the carboxylic and amino groups present on polysaccharides have already been modified by this strategy. Indeed, in a study by Aljawish (Aljawish et al., 2012), CN was functionalized by grafting ferulic acid (AF) oxidation products using *Myceliophthora thermophila* laccase. The authors showed

that the functionalization of CN was achieved on C2 by forming a Schiff base (the formation of a C=N bond was proven by FTIR analyses). Grafting of these phenolic oxidation products onto the carboxyl group was also studied on GA (Vuillemin et al., 2021). It was demonstrated that gum Arabic was grafted with oxidation products, close to the C6 of galactose units or close to the C5 of glucuronic acid units of gum Arabic. Furthermore, it was shown that the grafted products were mainly ferulic acid dimers, i.e. compounds with two aromatic rings, which could lead the modified polymers to establish new interactions such as π-π stacking or π-ion interactions. This strategy was implemented here to modify GA and CN. This paper aims to use these structure-modified polymers to contribute to the knowledge the formation of self-assembled colloidal systems. Thermodynamic parameters associated with the interactions were determined by Isothermal Titration Calorimetry (ITC). Measurements of Zeta potential and turbidity were compared to ITC results. These results were supported by microscopic observations to understand the mechanism of formation of the supramolecular structures.

2. Materials and Methods

2.1. Materials

Chitosan (CN) MMW (medium molecular weight, Mw 310 kDa verified by SEC-MALS experiments (Aljawish et al., 2014), deacetylation degree of 75%) was purchased from Sigma-Aldrich (France). Gum Arabic (GA) Instantgum AA from *Acacia senegal* (Mw 333 kDa determined by SEC-MALS experiments (Vuillemin et al., 2021)) was a gift from Nexira (France). Ferulic acid >99% (FA) was purchased from Sigma-Aldrich (France). Acetone, methanol and ethanol were purchased from Carlo Erba (France). Acetic acid, NaOH and ultrapure water were of analytical grade. The enzyme used for the modification of the polymers was commercialized as "Novozym® 51003" from Novozymes (Bagsvaerdt, Denmark). It is a

145 fungal laccase from *Myceliophthora thermophila*, a polyphenol oxidase. The laccase stock
146 activity was 32 038 ± 1 322 LAMU.g^{-1}.

147

148 ## 2.2. Methods

149 ### 2.2.1. Polymers modification

150 The functionalization of gum Arabic (GA) and chitosan (CN) was performed according
151 to the standard procedure of our laboratory (Aljawish et al., 2012; Vuillemin et al., 2020, 2021).
152 For chitosan (CN), the method was adapted from Aljawish et al. (Aljawish et al., 2012). For
153 gum Arabic (GA), the method was the same as that used by Vuillemin et al. (Vuillemin et al.,
154 2020, 2021). Briefly, 1 g of polysaccharide was dispersed in 45 mL of phosphate buffer
155 (50 mM, pH 7.5) and stirred at 4 °C overnight. Since the polysaccharides were not soluble in
156 this buffer, functionalization was performed under heterogeneous conditions. The dispersion
157 was stirred at 450 rpm for 1 h at 30 °C. 5 mL of ferulic acid dissolved in methanol (50 mM)
158 was added to the batch. Once the temperature was stable, 13.5 UI.mL^{-1} of Novozym® 51003
159 was added to trigger the reaction. The batch was then stirred at 30 °C for 50 min.

160 For chitosan (CN), the reaction was stopped by filtration of the reaction medium under
161 vacuum with Ministar-RC membranes (Sartorius, porosity 0.2 µm). The recovered
162 functionalized chitosan (FCN) was washed with phosphate buffer pH 7.5, ultrapure water,
163 methanol, ethanol and then acetone to remove all traces of substrates and enzyme on the
164 chitosan derivative.

165 For gum Arabic (GA), the reaction was stopped by adding 150 mL of cold ethanol. The
166 unfunctionalized GA precipitated. The resulting mixture of functionalized GA (FGA) and

ungrafted FA oxidation products (OXP) soluble in the phosphate buffer/ethanol mixture and insoluble unfunctionalized GA was then centrifuged for 20 min at 12000 *g* with a Beckmann centrifuge (Beckman Coulter Inc., Villepinte, France). The precipitate contained unfunctionalized GA (verified by FTIR measurements) and some of the phosphate buffer salts, whereas the supernatant contained the functionalized GA and the non-GA-grafted ferulic acid oxidation products. Ethanol was then removed using a BUCHI R144 rotary evaporator (BUCHI SARL, Rungis, France) at a boiling temperature of 40 °C under 175 mbar. Some water in the buffer solution was also evaporated by decreasing the pressure to 72 mbar.

The functionalized polysaccharides were frozen and then lyophilized for 72 h. The resulting powders were stored in a desiccator until use.

2.2.2. Polymers purification

Native chitosan (NCN), functionalized chitosan (FCN), native gum Arabic (NGA) and functionalized gum Arabic (FGA) were dialyzed against acetic acid (1% v/v) and water, respectively. A high-grade quality regenerated membrane (MWCO 10 000 Da from Membrane Filtration Products Inc.) was used to remove excess salts and possibly ungrafted FA oxidation products (OXP). Dialysis was stopped when the conductivity outside the membrane was equal to the one of acetic acid (1% v/v) or ultrapure water. The samples were then centrifuged for 30 min at 12,000 *g* to remove insoluble material and air bubbles and then freeze-dried and stored at 4 °C. The molecular weights of the two polysaccharides were confirmed by SEC-MALS measurement after dialysis. Grafting of the oxidation products onto chitosan did not significantly alter its molecular weight (310 kDa). However, the functionalization of gum Arabic changed its molecular weight (333 kDa for NGA and 213 kDa for FGA) (Vuillemin et al., 2021).

2.2.3. Polymers stock solutions preparation

Stock solutions of 0.02% w/v NCN and FCN ($6.45x10^{-4}$ mM) and 0.50% w/v NGA and FGA ($1.49x10^{-2}$ mM and $2.35x10^{-2}$ mM, respectively) were prepared by dissolving purified NCN and FCN or NGA and FGA in acetic acid (1% v/v in ultrapure water). The solutions were stirred on a magnetic plate at 400 rpm overnight at 4 °C to ensure that the polymers were completely dissolved. The NCN and FCN solutions were prepared at 0.02% w/v ($6.45x10^{-4}$ mM), a concentration for which its viscosity was low and suitable for ITC experiments. The concentration of NGA and FGA was adjusted to 0.50% w/v ($1.49x10^{-2}$ mM and $2.35x10^{-2}$ mM, respectively) based on preliminary measurements to optimize the concentrations for complete titration without signal saturation.

2.2.4. Polymers mixtures preparation

The polymer mixtures were prepared at 45 °C, pH 5.5 by adding acetic acid (1 N) or NaOH (5 N) as required, and different molar ratio of polymers. The required amount of polymer solutions was placed 15 min in a thermostatic degassing chamber (TA instruments, Waters SAS, France) to reach the target temperature and remove bubbles. The NGA or FGA solutions were then added to the NCN or FCN solutions.

2.2.5. Isothermal titration calorimetry (ITC)

ITC measurements were performed with an Affinity ITC equipped with a standard volume (965 µL) gold cell (TA instruments, Waters SAS, France) to measure the dissociation constant (K_d) and the enthalpic change due to the interaction between CN and GA. The entropy and the Gibbs free energy were obtained from the following equations:

$$\Delta G = - R.T.\ln(1/K_d) \qquad \text{(Eq. 1)}$$

$$T.\Delta S = \Delta H - \Delta G \quad \text{(Eq. 2)}$$

With ΔG: Gibbs free energy variation ($kJ.mol^{-1}$), ΔH: enthalpy variation ($kJ.mol^{-1}$), ΔS: entropy variation ($kJ.mol^{-1}.K^{-1}$), T: temperature (K) and R is the specific gas constant (8.3144598 $J.mol^{-1}.K^{-1}$).

Ultrapure water was used in the reference cell. The injector microsyringe (320 µL), was loaded with NGA or FGA stock solution (0.50% w/v NGA or FGA ($1.49x10^{-2}$ mM and $2.35x10^{-2}$ mM, respectively) in 1.00% v/v acetic acid solution). 5 µL was sequentially injected 50 times every 300 s into the titration cell filled with NCN or FCN solution (0.02% w/v NCN or FCN ($6.45x10^{-4}$ mM) in 1.00% v/v acetic acid solution). At the end of the experiment, the molar ratio of the mixture in the cell was 8.7:1 for the mixture with NGA and 13.6:1 for the mixture with FGA. The polymer concentrations were chosen based on preliminary measurements to optimize the concentrations for complete titration without signal saturation. For each measurement, the pH, temperature and acetic acid solvent were the same in the cell and in the syringe to limit the dilution effect. The heat of dilution from the blank titration was subtracted from the raw data in all experiments. Data acquisition was performed using ITC Run software and data were analyzed with the NanoAnalyse software (TA instruments, Waters SAS, France). The "Independent" model was selected as the most robust model from the plot residuals to fit the obtained isotherms. All measurements were performed in triplicate.

2.2.6. Approximate Zeta potential

The approximate Zeta potential of the polymers alone (0.02 w/v for NCN and FCN ($6.45x10^{-4}$ mM) and 0.50% w/v for NGA and FGA ($1.49x10^{-2}$ mM and $2.35x10^{-2}$ mM, respectively)) and mixtures was calculated from electrophoretic mobility measurements at controlled temperature (45 °C) using a Zetasizer Nano-ZS instrument (Malvern Panalytical,

UK) equipped with a He/Ne ion laser (λ= 532 nm). The measurements were collected on a detector at 173°. The instrument determined the Zeta potential with the Smoluchowski equation (Jayme et al., 1999). All measurements were performed in triplicate.

2.2.7. Turbidity measurements

Turbidity of the mixtures was measured with a UV-visible spectrophotometer (Shimadzu 1280, Japan) at 660 nm. The transmittance (T) of the spectrophotometer was calibrated with 0.1 N acetic acid to 100% and the turbidity of the samples was reported as 100-T%. The relative turbidity (τ) was calculated from the equation 3:

$$\tau = -\frac{1}{L}\ln\frac{I_0}{I_t} \qquad \text{(Eq. 3)}$$

Where L was the optical path length (1 cm) and I_t and I_0 represented the transmitted light intensity and the incident light intensity, respectively. All measurements were made in triplicate.

2.2.8. Optical microscopy

The mixtures were observed by optical microscopy (Olympus BH2, Japan) at x40 magnification. They were observed as prepared, i.e. without dilution of the samples. The images were recorded with a 5 MPixel CMOS camera (Olympus) under the control of ToupView software. The micrographs presented are representative of the samples.

2.2.9. Statistical analysis

Values were expressed as mean ± standard deviation. Differences between mean values were evaluated using one-way analysis of variance (ANOVA), which was performed with

Excel for Statistical Analysis and XLSTAT. Differences were considered statistically significant when the p_{value} was less than 0.05.

3. Results and discussion

3.1. Influence of polymer modification over their approximate Zeta potentials

Since coacervation is assumed to be primarily driven by electrostatic interactions, the influence of pH on polymer behavior was first investigated.

According to Table 1, native and modified polysaccharides were charged at pH 5.5 and 45 °C. Grafting of the oxidation products did not change the approximate Zeta potential of CN in acetic acid solution (17.4 ± 0.7 mV for NCN and 18.1 ± 0.2 mV for FCN). The grafted oxidation products were mainly ferulic acid dimers grafted onto the amine groups of chitosan (Aljawish et al., 2012, 2014). With positive charges of the amine groups replaced by oxidation products, the charge of the polymer would be expected to decrease. The approximate Zeta potential of CN at pH 3.0 was different between NCN and FCN (71.3 ± 2.8 mV and 62.5 ± 0.4 mV at 25 °C, respectively) confirming the grafting. These results are consistent with those obtained by Aljawish et al. (Aljawish et al., 2012). Nevertheless, at pH 3.0, neither NGA nor FGA were charged. Therefore, it was preferred to work at pH 5.5 so that each polymer was charged. The difference in Zeta potential observed between NCN and FCN at pH 3.0 was already small (12 %). Since at pH 5.5 the charge of NCN and FCN was lower, due to a pH close to their pKa (6.3), the influence of the grafting on the charge of the polymer was less marked and may enter into instrumental errors, explaining why no significant difference was observed. Furthermore, at the selected temperature and pH (45 °C, pH 5.5), the hydrodynamic radius of chitosan in solution was higher than under standard conditions (room temperature) and the

flexibility of the chains increased (Chen & Tsaih, 1998; Fan et al., 2012). Thus, under the conditions studied (pH close to the pKa of chitosan and temperature of 45 °C), the lack of charge difference between NCN and FCN could also be attributed to chain flexibility.

Table 1: Approximate Zeta potential of native chitosan (NCN, 0.02% w/v), functionalized chitosan (FCN, 0.02% w/v), native gum Arabic (NGA, 0.50% w/v) and functionalized gum Arabic (FGA, 0.50% w/v) solutions in acetic acid 1.00% v/v at pH 5.5, 45 °C. "a, b, and c" mean that the statistical analysis showed no significant differences between the results.

Approximate Zeta Potential (mV)			
NCN 0.02% w/v in acetic acid	FCN 0.02% w/v in acetic acid	NGA 0.50% w/v in acetic acid	FGA 0.50% w/v in acetic acid
17.4 ± 0.7^{a}	18.1 ± 0.2^{a}	-9.7 ± 0.7^{b}	-21.7 ± 1.1^{c}

According to Table 1, the charge of FGA was twice as high as that of NGA. Indeed, the oxidation products were mainly composed of ferulic acid dimers and trimers that were potentially negatively charged causing an increase in the negative charge of the polysaccharide after grafting (Vuillemin et al., 2021).

Many authors have previously reported that charge stoichiometry between NGA and NCN (when all NCN charges were neutralized by all NGA charges) was achieved for a composition of five times more NGA than NCN (Butstraen & Salaün, 2014; Espinosa-Andrews et al., 2010, 2013; Vuillemin et al., 2019). The results in Table 1 suggested that since the modification did not change the surface charge of chitosan, the introduction of FCN instead of NCN into the mixture should not change the stoichiometry. However, since the surface charge of FGA was twice that of NGA, it appeared that twice the amount of FGA compared to NGA would be required to neutralize chitosan charges and achieve stoichiometry.

To confirm that more FGA than NGA was needed to achieve stoichiometry and to shed light on the thermodynamic pathways of complex formation, whether the polymer was modified or not, ITC measurements were performed.

3.2. Influence of the polymers modification on the thermodynamic parameters involved in the complexation process

The influence of the modification of gum Arabic and chitosan structures over the thermodynamic parameters involved in the interaction process was studied using ITC at pH 5.5 and 45 °C.

The corrected heat rates recorded after each gum Arabic injection were predominantly negative in all cases (Figure 1A). This means that the major contribution of the interaction was mainly exothermic and that the interactions were spontaneous. Each peak corresponded to the energy released by the interaction between chitosan and gum Arabic after each injection. Initially, typical titration curves were observed. The intensities of the exothermic peaks decreased as a function of molar ratios until they stabilized. This stabilized sequence, related to a dilution phenomenon, corresponded to exothermic peaks. Furthermore, endothermic peaks were also observed at the end of the titration just after each exothermic peak. These phenomena were observed for all mixtures except the FGA/FCN mixture, for which no exothermic peaks were observed at the end of titration, only relatively high endothermic peaks. It is clear that the exothermic peaks are mainly related to the electrostatic interaction between the polymers (Priftis et al., 2012; Duhoranimana et al., 2018; Vuillemin et al., 2019). Solvent reorganization also accounts for a significant part of the exothermic signal, with extensive hydrogen bonding networks at the complex interface making the enthalpy change more favorable, even if

321 counterbalanced by an entropy penalty (endothermic peaks) (Turgeon et al., 2007). The
322 complexes were formed until the charges were neutralized.

323

324

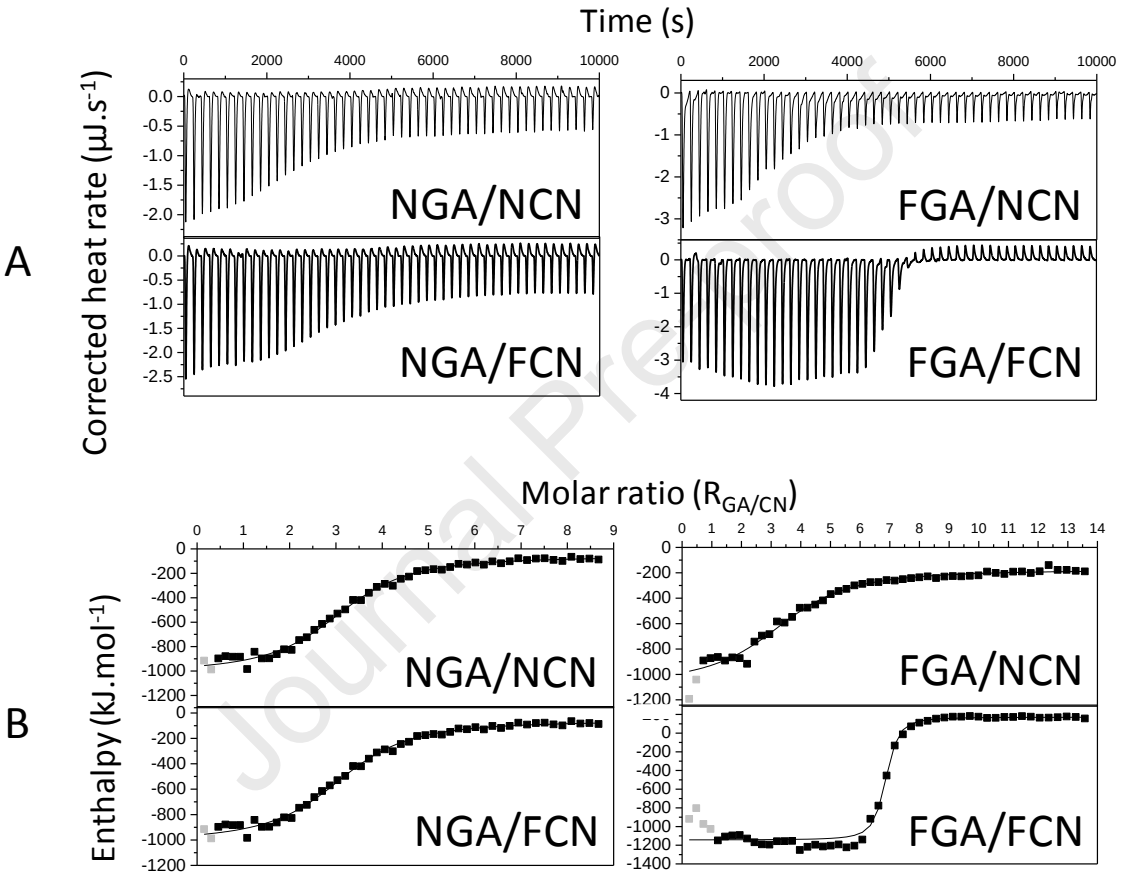

325

326 Figure 1: (A) Corrected heat rate upon time of mixtures between native gum Arabic (NGA) or
327 functionalized gum Arabic (FGA) and native chitosan (NCN) or functionalized chitosan (FCN)
328 at pH 5.5 at 45 °C. (B) Enthalpy and fit upon gum Arabic/chitosan molar ratio of mixtures
329 between native gum Arabic or functionalized gum Arabic and native chitosan or functionalized
330 chitosan at pH 5.5 at 45 °C. Grey points recorded at the beginning of the titration were excluded
331 from the fit.

332 The endothermic peaks at the end of the titration could be related either to aggregation,
333 reorganization within the system, or hydrophobic interactions (Kayitmazer, 2017; Weinbreck
334 et al., 2004). Indeed, the endothermic peaks with the highest intensities were observed when

335 FCN was present in the mixtures. Both NGA and FGA had hydrophobic moieties from the
336 protein fraction or grafted moieties, whereas NCN did not. Grafting of phenolic compounds
337 onto chitosan provided hydrophobic moieties capable of exhibiting novel interactions with
338 NGA and FGA.

339 Finally, the successive appearance of exothermic and endothermic signals is typical of
340 ITC measurements on complex formation for many systems (Turgeon et al., 2007). It has been
341 shown to be induced either by other energetic contributions such as the release of water
342 molecules and ions, by conformational changes of polysaccharides, by the aggregation of
343 polymer complexes or to the different steps involved in coacervation (Gonçalves et al., 2005;
344 Harnsilawat et al., 2006; Ziegler & Seelig, 2004; Hadian et al., 2016). The absence of
345 exothermic peaks at the end of the FGA/FCN titration could mean that these phenomena did
346 not occur in this system when gum Arabic was in excess, or be related to a reorganization
347 phenomenon of the system.

348 The binding isotherms were fitted using an "Independent" model (Figure 1B). This model
349 was used to determine the thermodynamic parameters involved in the interactions such as
350 dissociation constant, interaction enthalpy and stoichiometry. The enthalpy upon molar ratio
351 followed a typical titration curve. The interaction stoichiometry (n) corresponds to the inflection
352 point of the sigmoid curve. As it changed upon mixture, the stoichiometry is clearly not the
353 same. The enthalpy was also different upon mixture, which means that the thermodynamic
354 parameters were also different for the conditions studied. The free energy and thermo-entropic
355 contribution were calculated from Eq. 1 and Eq. 2. The results obtained are presented in Table
356 2.

357 Table 2: Thermodynamic parameters (dissociation constant (Kd), stoichiometry (n), enthalpic
358 contribution (ΔH), thermo-entropic contribution (TΔS) and Gibbs free energy (ΔG)) of binding
359 between native gum Arabic (NGA)/functionalized gum Arabic (FGA) and native chitosan

360 (NCN)/functionalized chitosan (FCN). “a, b and c” mean that the statistical analysis showed no
361 significant differences between the results, for each column. Results with the same letter means
362 there was no significant difference between them.

363

Mixtures	Kd.10^{-08}	n	ΔH (kJ.mol^{-1})	TΔS (kJ.mol^{-1})	ΔG (kJ.mol^{-1})
NGA NCN	14.5 ± 0.6^{a}	2.7 ± 0.2^{a}	-965.2 ± 40.7^{a}	-923.6 ± 40.9^{a}	-41.6 ± 0.2^{a}
NGA FCN	13.6 ± 5.3^{a}	3.1 ± 0.2^{ab}	-916.3 ± 48.8^{a}	-874.3 ± 47.7^{a}	-42.0 ± 1.1^{a}
FGA NCN	17.7 ± 6.9^{a}	3.4 ± 0.3^{b}	-913.3 ± 14.7^{a}	-872.2 ± 13.7^{a}	-41.1 ± 1.0^{a}
FGA FCN	0.4 ± 0.2^{b}	6.3 ± 0.6^{c}	-1331.5 ± 23.3^{b}	-1280.4 ± 24.5^{b}	-51.1 ± 1.2^{b}

364

365 For all conditions, the ΔG was always negative, meaning that self-assembly was always
366 spontaneous whether the polysaccharides were functionalized or not. The K_d values were
367 always low (from 0.4 x 10^{-8} to 17.7 x 10^{-8}) corresponding to strong interactions (an interaction
368 is considered strong when the K_d value is less than 10^{-6} (Qin & Gronenborn, 2014)). The K_d
369 value was lower for the FGA/FCN mixture. This could mean that the strength of the interaction
370 was greater when both polymers were functionalized. This could potentially be related to the
371 increased charge of FGA in comparison to NGA and to the grafting of the oxidation product
372 onto gum Arabic and chitosan, which could promote further interactions between them.

373 The ΔH values were negative in all cases, as were the TΔS values. The ΔH values, mainly
374 related to electrostatic interactions (Aberkane et al., 2010; Kayitmazer, 2017; Vuillemin et al.,
375 2019), are considered favorable to interactions when they are negative (negative contribution
376 to ΔG, see Eq.1). On the contrary, the values of TΔS, related to hydrophobic interactions
377 (Kayitmazer, 2017; Weinbreck et al., 2004), are favorable to interactions when they are
378 positive. In the given cases, ΔH values were always favorable to interactions (from - 913.3 ±

379 14.7 kJ.mol^{-1} to - 1331.5 ± 23.3 kJ.mol^{-1}) and TΔS values were always unfavorable to
380 interactions (from - 872.2 ± 13.7 kJ.mol^{-1} to -1280.4 ± 24.5 kJ.mol^{-1}).

381 Regarding the stoichiometry values (Table 2), the involvement of FGA may have resulted in a
382 change in stoichiometry. For mixtures containing NGA, the stoichiometry was the same (2.7 ±
383 0.2 for NGA/NCN mixtures and 3.1 ± 0.2 for NGA/FCN mixtures). However, for mixtures
384 containing FGA, the stoichiometry was different (3.4 ± 0.3 for FGA/NCN mixtures and 6.3 ±
385 0.6 for FGA/FCN mixtures). The difference between mixtures containing NGA and FGA was
386 expected from the change in the approximate Zeta potential of gum Arabic after
387 functionalization (Table 1). However, the difference in stoichiometry observed between the
388 FGA/NCN and FGA/FCN mixtures (3.4 ± 0.3 and 6.3 ± 0.6, respectively) was surprising,
389 because the approximate Zeta potential of chitosan was the same at pH 5.5 after
390 functionalization. This result suggests that electrostatic interactions are not the only types of
391 interactions between the two modified polymers. This could indicate that when both polymers
392 were modified, potential hydrophobic interactions, π-π stacking, cation-π and anion-π induced
393 by the grafting of phenolic compounds could lead to a change in complexation stoichiometry
394 and an increase in polymer content. However, hydrophobic interactions would mainly lead to
395 aggregation, as already studied by Kaibara (2000) on the elastin/water system (Kaibara et al.,
396 2000). While the ΔG was almost the same for all conditions examined, it was significantly more
397 negative for FGA/FCN mixture (-51.1 ± 1.2 kJ.mol^{-1}). Furthermore, this mixture had the lowest
398 K_d (0.4x10^{-8} ± 0.2x10^{-8}), which means that under these conditions the interaction between
399 modified gum Arabic and modified chitosan was the most favorable.

400 The enthalpic and entropic parameters did not change whether chitosan was functionalized or
401 not (Table 2). However, the functionalization of both polymers had an impact on them. ΔH
402 varied from -965.2 ± 40.7 kJ.mol^{-1} for NGA/NCN mixtures to -1331.5 ± 23.3 kJ.mol^{-1} for

FGA/FCN mixture while TΔS varied from -923.6 ± 40.9 kJ.mol^{-1} to -1280.4 ± 24.5 kJ.mol^{-1}, respectively. This means that the enthalpy contribution became more favorable to the interaction while the entropy contribution became less favorable when both polymers were modified. This makes sense, as the functionalization of gum Arabic, while increasing its hydrophobicity and/or the possibility for it to undergo π-π stacking, cation-π and anion-π interactions, increased its negative charges, likely leading to more electrostatic interaction.

A surprising result was obtained from the comparison of the enthalpic and entropic contributions of FGA/NCN and FGA/FCN. Since the charges of chitosan were the same whether it was functionalized or not, the observed difference could not be explained by an increase in electrostatic interaction. However, although the thermodynamic parameters did not indicate a significant role of hydrophobic interactions in the complexation process, the isotherms (Figure 1A) showed an endothermic contribution at the end of the titration. This could mean that in the case of FGA/FCN mixtures, there could be a competition between electrostatic interactions, which are strong at the beginning of the titration until stoichiometry is reached, and hydrophobic interactions, which are predominant at the end of the titration.

By measuring the approximate Zeta potential upon polymers molar ratio, the turbidity of the samples after mixing and with the support of optical microscopy, a more thorough understanding of the type of interactions that were occurring should be gained in order to elucidate the complexation mechanism.

3.3. Characteristics of polymer mixtures upon molar ratio

The influence of the molar ratio on the approximate Zeta potential and turbidity of the samples was studied for each potential mixture (Figure 2). The experiments were performed at pH 5.5, 45 °C. Measurements and observations were performed 5 min after mixing the polymers solutions.

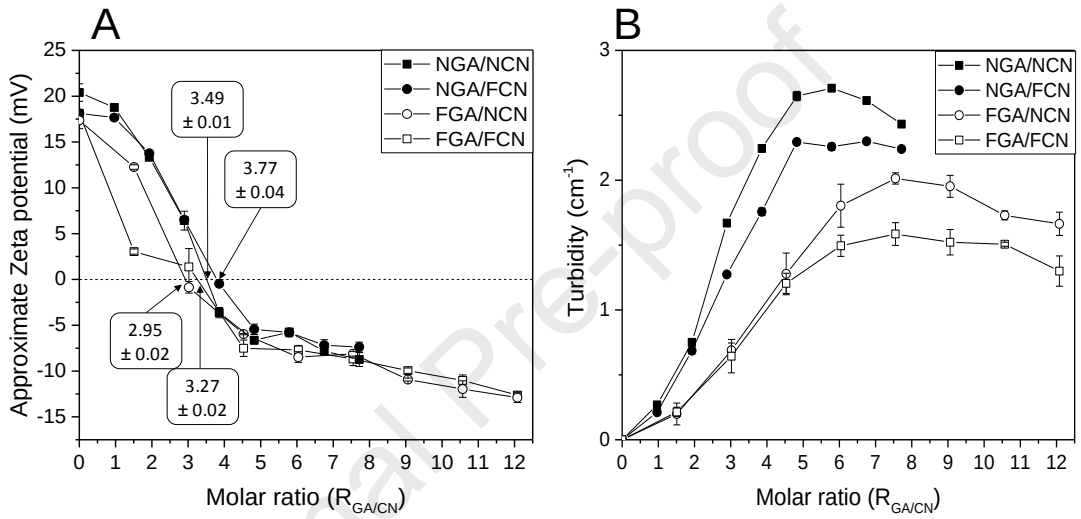

Figure 2: (A) Approximate Zeta potential (mV) and (B) turbidity (cm^{-1}), of mixtures between native gum Arabic (NGA) or functionalized gum Arabic (FGA) and native chitosan (NCN) or functionalized chitosan (FCN) upon gum Arabic/chitosan molar ratio at pH 5.5 and 45 °C, 5 min after mixing.

When mixing gum Arabic and chitosan, the approximate Zeta potential decreased upon addition of gum Arabic (Figure 2A). This is because the charges of chitosan (NCN or FCN) were progressively neutralized upon addition of FGA or NGA to the mixtures. The molar ratio for which the approximate Zeta potential of the mixture was zero was not exactly the same as the stoichiometry obtained by ITC measurements (Table 2), but similar trends were reported for all mixtures except for the FGA/FCN mixture. The optimal molar ratio (for which charges

were neutralized) was lower by Zeta potential measurements than by ITC measurements for FGA/FCN mixtures (3.27 ± 0.02 versus 6.3 ± 0.6, respectively). This means that the optimal molar ratio obtained by ITC for FGA/FCN interaction was not simply due to electrostatic interactions. This confirmed that other types of interactions such as π-π stacking, cation-π and anion-π were at work for this mixture at 45 °C.

Upon molar ratio, the turbidity of the mixtures increased up to a molar ratio of 4.9:1 for the mixtures containing NGA and 7.6 for mixtures containing FGA, then decreased slightly (Figure 2B). For molar ratio lower than these, the turbidity was different for the different mixtures, indicating the formation of various supramolecular structures (coacervates or aggregates of different size and shape). These differences may be related to the shape of the formed samples, as can be seen in Figure 3.

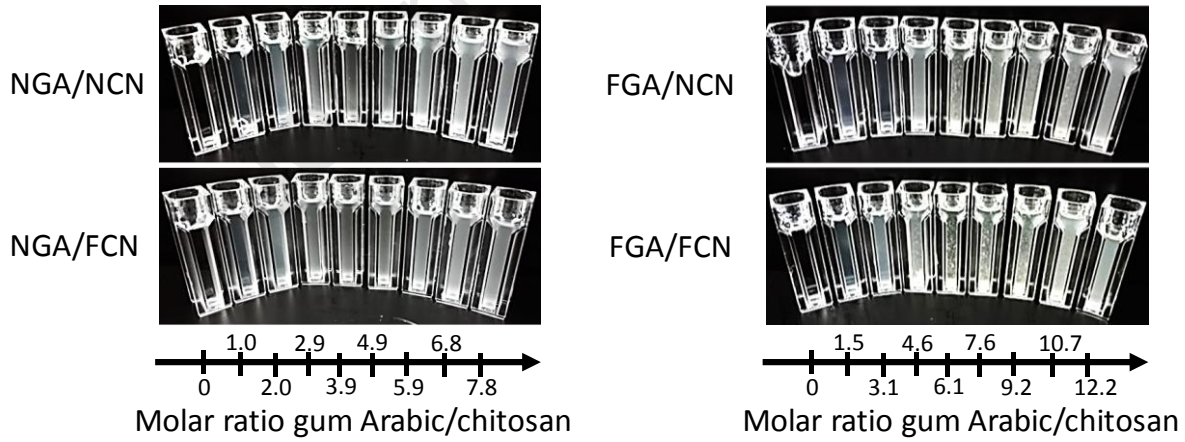

Figure 3: Macroscopic observations of mixtures between native gum Arabic (NGA) or functionalized gum Arabic (FGA) and native chitosan (NCN) or functionalized chitosan (FCN) mixtures upon molar ratio at 45 °C, 5 min after mixing.

From the macroscopic observation in Figure 3, it can be observed that the mixtures exhibited different behavior depending on the polymers involved and the molar ratio. Some

458 samples appeared “homogeneously” turbid while aggregates were observed on others. Mixtures
459 containing NGA were turbid while the presence of FGA seemed to lead to the formation of
460 aggregates at certain molar ratios. In the photographs of the mixtures (Figure 3), it would appear
461 that the mixtures become more turbid for NGA/NCN and NGA/FCN mixtures upon molar
462 ratios. However, for mixtures containing FGA, the mixtures became turbid upon FGA addition
463 until a molar ratio was reached when aggregation occurred (for ratio 3.1 for FGA/FCN mixtures
464 and for the 6.1 ratio for FGA/NCN mixtures). To confirm the presence of coacervates and
465 aggregates in the samples, the mixtures were observed by optical microscopy (Figure 4).

466

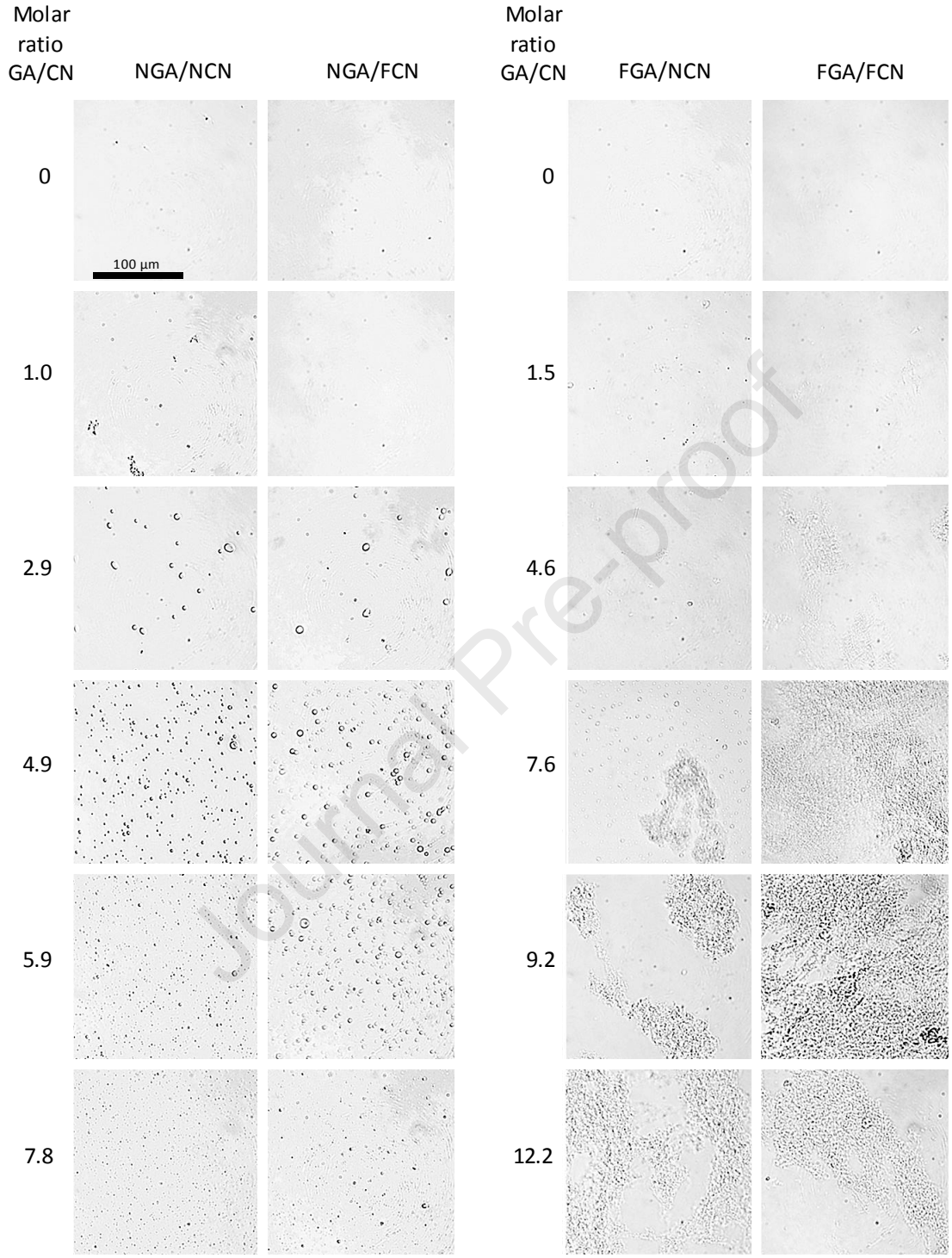

467

468 Figure 4: Optical micrographs of mixture between native gum Arabic (NGA) or functionalized
469 gum Arabic (FGA) and native chitosan (NCN) or functionalized chitosan (FCN) mixtures upon
470 different GA/CN molar ratios 5 min after mixing at 45 °C, pH 5.5.

For molar ratio below 1.0, no supramolecular structures were observed for all mixtures. When NGA was added to NCN or FCN up to a molar ratio of 2.9, a few coacervates appeared. They became more numerous for a molar ratio of 4.9. Upon addition of NGA, coacervates tended to disappear (molar ratio 7.8).

For FGA/NCN mixtures (Figure 4), no supramolecular structures were observed for a molar ratio of 7.6. For a molar ratio of 7.6, a coexistence of two types of supramolecular structures was observed: there were both coacervates and aggregates. Above a molar ratio of 9.2, no more coacervates were observed, but the aggregates became larger and more numerous. For FGA/FCN mixtures, no coacervates were observed at any molar ratio. However, aggregates started to appear for a molar ratio of 4.6, and they became larger until the molar ratio of 7.6 was reached. For a molar ratio of 9.2, it appears that the density of aggregates decreased. The latter result was positively correlated with the turbidity and macroscopic aspect of the mixtures (Figure 2 and Figure 3). This could be due to a reorganization within the different systems that would correlate with the endothermic events observed on ITC measurements above a molar ratio of 8 (Figure 1A). By linking the ITC measurements, the thermodynamic parameters obtained from fitting the raw data, to macroscopic observations, Zeta potential measurements, turbidity measurements and optical micrographs, a mechanism was proposed to explain what happened within the different systems.

3.4. Possible mechanism of the interaction between gum Arabic and chitosan

The interactions between NGA and NCN were electrostatic interactions between the carboxyl groups of gum Arabic and the amine groups of chitosan (Butstraen & Salaün, 2014; Espinosa-Andrews et al., 2007, 2010; Vuillemin et al., 2019). The two polymers attracted each

other due to their opposite charges, followed by the release of water and counterions. Then, upon addition of gum Arabic, the charges of the two polymers were balanced. Upon addition of gum Arabic beyond stoichiometry, reorganization of the complexes occurred until the complexes disintegrated to reach equilibrium in the systems (observed in previous studies on NCN and NGA (Vuillemin et al., 2019)).

Studies often agree that there is an initial step of soluble complexes formation prior to the actual coacervation step. Recent studies have focused on these complexes formed between oppositely charged polyelectrolytes as precursors to coacervates and multilayers (Comert et al., 2018). The presence of these small precursors has been reported to increase the turbidity of samples, and it has been suggested that this is related to an increase in the size or number of complexes or soluble aggregates. In the optical micrographs, for the first few molar ratios, even though no supramolecular structures were visible, it could be assumed that soluble complexes or soluble aggregates were formed, due to the increased turbidity of the samples (Figure 2 and Figure 3).

For the NGA/NCN system, up to a molar ratio of 1.0, no complexes were visible **(**Figure 4). However, it was possible that supramolecular structures had formed, but they were too small to be seen by optical microscopy. This was confirmed by the turbidity of the mixtures (Figure 2) rising before the first coacervates could be observed by optical microscopy (Figure 4). When mixed beyond a ratio of 2.9, these two oppositely charged polysaccharides began to form coacervates **(**Figure 4**)**. When more NGA was added to NCN, more charges of the polymers interacted. The stoichiometry value determined by ITC (2.7) was confirmed by optical microscopy (first supramolecular structures at 2.9), macroscopic observations (first turbid samples at 2.0) and Zeta potential (optimal ZP at 3.49). At ratio 7.8, when NGA was in excess, the complexes became smaller. To reach an equilibrium in the system, the GA could desorb

518 and the coacervates could change. This assumption was consistent with the small endothermic
519 event at the end of the titration (Figure 1). This could be explained by this reorganization within
520 the system.

521

522 For the NGA/FCN system, the same phenomena were observed **(**Figure 4**)**. The ITC
523 results, macroscopic and microscopic observations as well as Zeta potential and turbidity
524 indicated no change when replacing NCN with FCN. This means that the coacervation process
525 was probably the same. Since the charges of FCN and NCN were the same at the chosen pH
526 and temperature, the interactions between FCN and NGA were likely mainly electrostatic
527 interactions. If another phenomenon occurred, such as hydrophobic interactions or π-anion
528 interactions between NGA and the grafted oxidation products of FCN, the experiments did not
529 reveal them.

530

531 For the FGA/FCN system, no coacervation phenomena were clearly observed in
532 photographs of the sample or in micrographs **(**Figure 3 and Figure 4**)**. Up to a molar ratio of
533 3.1, the aspect of the sample became turbid but no supramolecular structures were visible by
534 optical microscopy. This means that before this ratio, small complexes were formed. After a
535 ratio of 4.6, aggregates appeared **(**Figure 4**)**. The optimal molar ratio determined by Zeta
536 potential measurements was consistent with the appearance of the turbidity (3.27) and the
537 appearance of aggregates was consistent with the optimal molar ratio determined by ITC (6.3).
538 This means that the formation of soluble complexes was primarily driven by electrostatic
539 interactions but the formation of aggregates would be driven by other forces. ITC parameters
540 confirmed that the presence of FGA and FCN increased the contribution of the enthalpic

parameter. This could be due to the fact that both polymers are grafted with oxidation products, which leads to more π-π stacking, π-cation and π-anion interactions increasing the enthalpic contribution. The presence of exothermic hydrophobic interactions could not be excluded, but their effect on the titration isotherms would probably be concealed by all the other interactions involved in the aggregation phenomenon. However, at the end of titration, hydrophobic interactions between FGA and FCN would be predominant (Figure 1).

The increased charge of FGA in comparison to NGA could increase the strength of its interactions with chitosan. It is widely accepted that strong attractive properties promote aggregation (Comert & Dubin, 2017). The polyelectrolyte structure also modulates the type of phase separation observed. Indeed, the structure of the modified polymers changed their steric hindrance, consequently modifying the accessibility of polysaccharides to each another. It was revealed in previous studies that the glass transition temperature of gum Arabic decreased upon functionalization, meaning that the grafting of phenolic compounds would have added to the steric hindrance of FGA and made its chains more flexible, allowing it to undergo more interactions (Vuillemin et al., 2020, 2021). The increase in FGA charge, leading to stronger electrostatic interactions, combined with increase in steric hindrance and the increase in polymer flexibility would be responsible for the aggregation phenomenon observed for the FGA/FCN mixtures.

For the FGA/NCN system, the turbidity of the sample increased after the addition of FGA (Figure 2). A slight difference was observed at a molar ratio of 1.5, but the turbidity was higher at a ratio of 4.6. At a molar ratio of 6.1, aggregates appeared (Figure 3). The optimal molar ratio obtained by Zeta potential measurements (2.95) and ITC measurements (3.4) were almost the same, but no supramolecular structures were visible by optical microscopy until a molar ratio

565 of 7.6. This means that before this ratio, soluble complexes were formed. However, at a ratio
566 of 7.6, two distinct phenomena were observed by macroscopic observations. Coacervates and
567 aggregates were present in the mixture. In the literature, the differentiation between the two
568 mechanisms is often obscured by the common use of turbidity to detect these transitions
569 (Comert & Dubin, 2017). Both mechanisms induce an increase in turbidity, but microscopy is
570 needed to know whether the turbidity arises from small soluble complexes, coacervation or
571 aggregation. By adding more FGA to the mixture, only aggregates were visible in the optical
572 micrographs.

573 A surprising result was the difference between the NGA/NCN mixture and the FGA/NCN
574 mixture. Indeed, the ITC results (Table 2) were not significantly different for these mixtures
575 and the stoichiometries were almost the same. However, turbidity showed the appearance of
576 aggregates for the FGA/NCN mixtures as well as the appearance of coacervates for a molar
577 ratio of 7.6 (Figure 3) which were confirmed by optical microscopy (Figure 4). Furthermore,
578 while the stoichiometry obtained by ITC was almost the same for NGA/NCN and FGA/NCN
579 mixtures, the stoichiometry obtained by approximate Zeta potential measurements was lower
580 for the FGA/NCN mixtures. This could be explained by the fact that a lower amount of FGA
581 was required to neutralize the charge of chitosan since FGA was more charged than NGA (Table
582 1). The fact that the charge stoichiometry and the one obtained by ITC were close (2.95 ± 0.02
583 and 3.4 ± 0.3, respectively) could explain why the two phenomena coexist for a molar ratio of
584 3.9 in the optical micrographs.

585

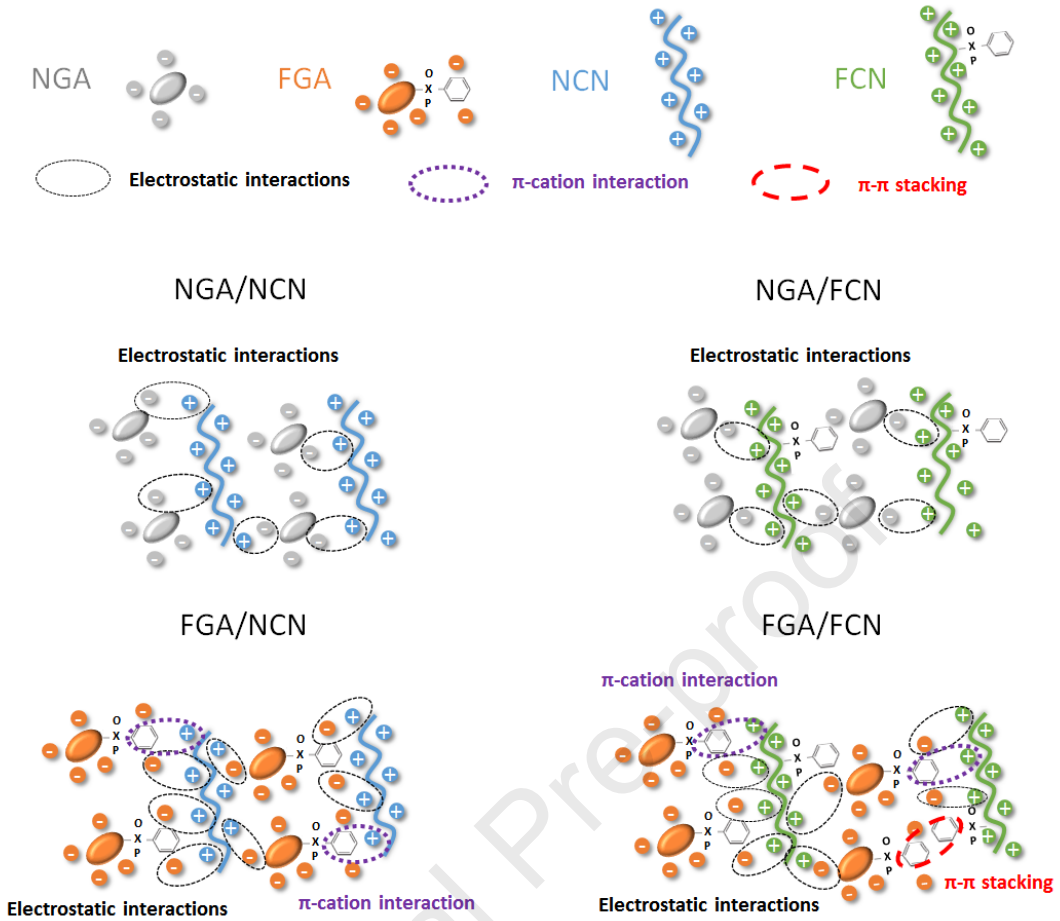

586

587 Figure 5: Schematic representation of the possible interactions between native gum Arabic
588 (NGA) or functionalized gum Arabic (FGA) and native chitosan (NCN) or functionalized
589 chitosan (FCN)

590 At the chosen pH and temperature, due to their charges under these conditions,
591 NGA/NCN and NGA/FCN exhibited typical « weakly charged polyelectrolytes » coacervation
592 behavior and steps, mainly driven by electrostatic interactions (negative enthalpy), with the
593 entropy of counterion release playing only a minor role (Turgeon et al., 2007). The fact that
594 these mixtures exhibited the same behavior suggests that mainly electrostatic interactions
595 occurred between NGA and NCN and NGA and FCN (Figure 5).

596 In the FGA/NCN system, several phenomena were observed. First, soluble complexes
597 were formed. Then, coacervates appeared as well as aggregates (Figure 4). Then, the
598 coacervates disappeared and only aggregates remained, meaning that stronger interactions were

599 present (Comert & Dubin, 2017). These were probably mainly more electrostatic interactions,
600 due to the higher charge of FGA, but they could also be due to π-cation interaction between the
601 amine groups of NCN and the phenol groups of the oxidation products grafted onto FGA
602 (Figure 5).

603 Based on the fact that coacervation usually occurs when the interactions are weak and on
604 the contrary, aggregation is a consequence of strong interactions, it might be surprising if
605 coacervation occurred before aggregation or at the same time. However, the strength of the
606 interactions should not be regarded as the sole strength of electrostatic and π-cation interactions
607 between one FGA and one NCN but has the number of interactions in the system. Though some
608 interactions are individually weak, they can become collectively important (Biedermann &
609 Schneider, 2016; Neel et al., 2017). One explanation for the coexistence of coacervation and
610 aggregation would be that the "collective importance" of the π-cation interactions between FGA
611 and NCN was low at a given molar ratio, leading to coacervation, and that when the molar ratio
612 increased, this "collective importance" increased with the amount of FGA aromatic rings,
613 leading to the disappearance of coacervates in favor of aggregates. Another explanation could
614 be based on the fact that chitosan opens the structure of FGA when they interact. This would
615 lead to exposure of FGA phenolic groups from the grafted oxidation products to the solvent,
616 which would decrease the affinity of the polymer for the aqueous solvent. This could lead to an
617 aggregation phenomenon.

618 For the FGA/FCN system, soluble complexes appeared to have been formed at the
619 beginning of the titration, but then only aggregates were visible. The strength of the interaction
620 was higher than for the other systems (Table 2) and the enthalpy was the most favorable in this
621 system. These stronger interactions could be due to FGA, as described for the FGA/NCN
622 system, but other interactions were involved since the results for the FGA/FCN system were

623 different from the ones for FGA/NCN systems. These interactions were not involved in the
624 mixtures containing NCN or NGA/NCN systems, meaning that they were due to the
625 modification of both FGA and FCN. These strong and numerous interactions would lead to
626 aggregation instead of coacervation. The aggregation phenomenon could be related to the fact
627 that both polymers were grafted with oxidation products, which leads to more π-π stacking and
628 π-cation interaction, thus increasing the enthalpic contribution (Figure 5). The increase in FGA
629 charge likely also contributed to enhanced electrostatic interactions. Similarly, the increase in
630 steric hindrance and the increase in polymer flexibility induced by grafting of phenolic
631 compounds onto the polymer is known to promote the aggregation phenomenon.

632

633 ## 4. Conclusions

634 This study provided a better understanding of the impact of the interaction balance
635 between two polymers on the formation of self-assembled structures. By comparing the
636 interaction stoichiometry (ITC results) and charge stoichiometry (approximate Zeta potential
637 results), it was shown that the interaction of chitosan with modified gum Arabic was not solely
638 due to electrostatic interactions. The strength of the interaction (K_d measured by ITC) was
639 higher for the mixture containing modified chitosan and modified gum Arabic, which meant
640 that other interactions occurred between those two (new π-π stacking and π-cation interactions).
641 The balance between these different interactions (their nature but also their collective strength)
642 led not only to the formation of coacervates but also to the formation of aggregates (confirmed
643 by turbidity measurements, macroscopic observation of the mixtures and optical microscopy).

644 By managing the physicochemical conditions of the medium and by judiciously choosing
645 the polymers (modified or not) it is possible to control the structures formed. Moreover, with

646 modified polymers, it is possible to form coacervates or aggregates under conditions different
647 from the optimal conditions with native polymers. With native polymers, to control the
648 structures formed, the physicochemical conditions of the medium must be controlled. When
649 these structures are used *in vivo* or to mimic the compartmentalized environments of cells for
650 example, the conditions of the medium are already fixed. The use of polymer modification
651 seems to be a promising way to control the structures formed in a given medium for
652 encapsulation purposes, for example.

653

654 Acknowledgments

655 The authors acknowledge support of the LIBio by the "Impact Biomolecules" project of
656 the "Lorraine Université d'Excellence" (Investissements d'avenir – ANR).

657 The authors acknowledge support of the CPER Agrovalor.

658 We would like to thank Nexira for kindly providing the gum Arabic used in this article.

659 We also thank Blandine Simard for the technical support.

660 References

661 Aberkane, L., Jasniewski, J., Gaiani, C., Scher, J., & Sanchez, C. (2010). Thermodynamic
662 characterization of acacia gum-beta-lactoglobulin complex coacervation. *Langmuir:*
663 *The ACS Journal of Surfaces and Colloids*, *26*(15), 12523–12533.
664 https://doi.org/10.1021/la100705d

665 Aljawish, A., Chevalot, I., Jasniewski, J., Paris, C., Scher, J., & Muniglia, L. (2014). Laccase-
666 catalysed oxidation of ferulic acid and ethyl ferulate in aqueous medium: A green
667 procedure for the synthesis of new compounds. *Food Chemistry*, *145*, 1046–1054.
668 https://doi.org/10.1016/j.foodchem.2013.07.119

669 Aljawish, A., Chevalot, I., Piffaut, B., Rondeau-Mouro, C., Girardin, M., Jasniewski, J., Scher,
670 J., & Muniglia, L. (2012). Functionalization of chitosan by laccase-catalyzed oxidation
671 of ferulic acid and ethyl ferulate under heterogeneous reaction conditions. *Carbohydrate*
672 *Polymers*, *87*(1), 537–544. https://doi.org/10.1016/j.carbpol.2011.08.016

673 Aumiller, W. M., Pir Cakmak, F., Davis, B. W., & Keating, C. D. (2016). RNA-Based
674 Coacervates as a Model for Membraneless Organelles: Formation, Properties, and
675 Interfacial Liposome Assembly. *Langmuir*, *32*(39), 10042–10053.
676 https://doi.org/10.1021/acs.langmuir.6b02499

677 Avadi, M. R., Sadeghi, A. M. M., Mohammadpour, N., Abedin, S., Atyabi, F., Dinarvand, R.,
678 & Rafiee-Tehrani, M. (2010). Preparation and characterization of insulin nanoparticles
679 using chitosan and Arabic gum with ionic gelation method. *Nanomedicine-*
680 *Nanotechnology Biology and Medicine*, *6*(1), 58–63.
681 https://doi.org/10.1016/j.nano.2009.04.007

682 Beppu, M. M., & Santana, C. C. (2002). Influence of Calcification Solution on in vitro Chitosan
683 Mineralization. *Materials Research*, *5*(1), 47–50. https://doi.org/10.1590/S1516-
684 14392002000100008

685 Biedermann, F., & Schneider, H.-J. (2016). Experimental Binding Energies in Supramolecular
686 Complexes. *Chemical Reviews*, *116*(9), 5216–5300.
687 https://doi.org/10.1021/acs.chemrev.5b00583

688 Bosnea, L., Moschakis, T., & Biliaderis, C. (2014). Complex Coacervation as a Novel
689 Microencapsulation Technique to Improve Viability of Probiotics Under Different
690 Stresses. *Food and Bioprocess Technology*, *7*(10), 2767–2781.
691 https://doi.org/10.1007/s11947-014-1317-7

692 Bosnea, L., Moschakis, T., & Biliaderis, C. G. (2017). Microencapsulated cells of Lactobacillus
693 paracasei subsp. Paracasei in biopolymer complex coacervates and their function in a
694 yogurt matrix. *Food & Function*, *8*(2), 554–562. https://doi.org/10.1039/c6fo01019a

695 Butstraen, C., & Salaün, F. (2014). Preparation of microcapsules by complex coacervation of
696 gum Arabic and chitosan. *Carbohydrate Polymers*, *99*, 608–616.
697 https://doi.org/10.1016/j.carbpol.2013.09.006

698 Campbell, N., & Reece, J. B. (2004). *Biology 7th Edition* (7th ed.).
699 https://www.pearson.ch/HigherEducation/BenjaminCummings/EAN/9780805371468/
700 Campbell-Biology-7th-Edition-

701 Chen, R. H., & Tsaih, M. L. (1998). Effect of temperature on the intrinsic viscosity and
702 conformation of chitosans in dilute HCl solution. *International Journal of Biological*
703 *Macromolecules*, *23*(2), 135–141. https://doi.org/10.1016/S0141-8130(98)00036-1

704 Coelho, S., Moreno-Flores, S., Toca-Herrera, J. L., Coelho, M. A. N., Carmo Pereira, M., &
705 Rocha, S. (2011). Nanostructure of polysaccharide complexes. *Journal of Colloid and*
706 *Interface Science*, *363*(2), 450–455. https://doi.org/10.1016/j.jcis.2011.07.098

707 Comert, F., & Dubin, P. L. (2017). Liquid-liquid and liquid-solid phase separation in protein-
708 polyelectrolyte systems. *Advances in Colloid and Interface Science*, *239*, 213–217.
709 https://doi.org/10.1016/j.cis.2016.08.005

710 Comert, F., Xu, A. Y., Madro, S. P., Liadinskaia, V., & Dubin, P. L. (2018). The so-called
711 critical condition for polyelectrolyte-colloid complex formation. *The Journal of*
712 *Chemical Physics*, *149*(16), 163321. https://doi.org/10.1063/1.5029296

713 Crowe, C. D., & Keating, C. D. (2018). Liquid–liquid phase separation in artificial cells.
714 *Interface Focus*, *8*(5), 20180032. https://doi.org/10.1098/rsfs.2018.0032

715 Drobot, B., Iglesias-Artola, J. M., Le Vay, K., Mayr, V., Kar, M., Kreysing, M., Mutschler, H.,
716 & Tang, T.-Y. D. (2018). Compartmentalised RNA catalysis in membrane-free
717 coacervate protocells. *Nature Communications*, *9*(1), 1–9.
718 https://doi.org/10.1038/s41467-018-06072-w

719 Duhoranimana, E., Yu, J., Mukeshimana, O., Habinshuti, I., Karangwa, E., Xu, X., Muhoza,
720 B., Xia, S., & Zhang, X. (2018). Thermodynamic characterization of Gelatin–Sodium
721 carboxymethyl cellulose complex coacervation encapsulating Conjugated Linoleic
722 Acid (CLA). *Food Hydrocolloids*, *80*, 149–159.
723 https://doi.org/10.1016/j.foodhyd.2018.02.011

724 Espinosa-Andrews, H., Báez-González, J. G., Cruz-Sosa, F., & Vernon-Carter, E. J. (2007).
725 Gum Arabic−Chitosan Complex Coacervation. *Biomacromolecules*, *8*(4), 1313–1318.
726 https://doi.org/10.1021/bm0611634

727 Espinosa-Andrews, H., Enríquez-Ramírez, K. E., García-Márquez, E., Ramírez-Santiago, C.,
728 Lobato-Calleros, C., & Vernon-Carter, J. (2013). Interrelationship between the zeta
729 potential and viscoelastic properties in coacervates complexes. *Carbohydrate Polymers*,
730 *95*(1), 161–166. https://doi.org/10.1016/j.carbpol.2013.02.053

731 Espinosa-Andrews, H., Sandoval-Castilla, O., Vázquez-Torres, H., Vernon-Carter, E. J., &
732 Lobato-Calleros, C. (2010). Determination of the gum Arabic–chitosan interactions by
733 Fourier Transform Infrared Spectroscopy and characterization of the microstructure and
734 rheological features of their coacervates. *Carbohydrate Polymers*, *79*(3), 541–546.
735 https://doi.org/10.1016/j.carbpol.2009.08.040

736 Fan, W., Yan, W., Xu, Z., & Ni, H. (2012). Formation mechanism of monodisperse, low
737 molecular weight chitosan nanoparticles by ionic gelation technique. *Colloids and*
738 *Surfaces B: Biointerfaces*, *90*, 21–27. https://doi.org/10.1016/j.colsurfb.2011.09.042

739 Fathi, M., Martín, Á., & McClements, D. J. (2014). Nanoencapsulation of food ingredients
740 using carbohydrate based delivery systems. *Trends in Food Science & Technology*,
741 *39*(1), 18–39. https://doi.org/10.1016/j.tifs.2014.06.007

742 Gonçalves, E., Kitas, E., & Seelig, J. (2005). Binding of Oligoarginine to Membrane Lipids and
743 Heparan Sulfate: Structural and Thermodynamic Characterization of a Cell-Penetrating
744 Peptide. *Biochemistry*, *44*(7), 2692–2702. https://doi.org/10.1021/bi048046i

745 Hadian, M., Hosseini, S. M. H., Farahnaky, A., Mesbahi, G. R., Yousefi, G. H., & Saboury, A.
746 A. (2016). Isothermal titration calorimetric and spectroscopic studies of β-lactoglobulin-
747 water-soluble fraction of Persian gum interaction in aqueous solution. *Food*
748 *Hydrocolloids*, *55*, 108–118. https://doi.org/10.1016/j.foodhyd.2015.11.006

749 Harnsilawat, T., Pongsawatmanit, R., & McClements, D. J. (2006). Characterization of β-
750 lactoglobulin–sodium alginate interactions in aqueous solutions: A calorimetry, light
751 scattering, electrophoretic mobility and solubility study. *Food Hydrocolloids*, *20*(5),
752 577–585. https://doi.org/10.1016/j.foodhyd.2005.05.005

753 Huang, G.-Q., Han, X.-N., & Xiao, J.-X. (2017). Glutaraldehyde-crosslinked O-carboxymethyl
754 chitosan–gum Arabic coacervates: Characteristics versus complexation acidity. *Journal*
755 *of Dispersion Science and Technology*, *38*(11), 1607–1612.
756 https://doi.org/10.1080/01932691.2016.1265454

757 Huang, G.-Q., Xiao, J.-X., Jia, L., & Yang, J. (2015). Complex Coacervation of O-
758 Carboxymethylated Chitosan and Gum Arabic. *International Journal of Polymeric*
759 *Materials and Polymeric Biomaterials*, *64*(4), 198–204.
760 https://doi.org/10.1080/00914037.2014.936591

761 Huang, G.-Q., Xiao, J.-X., Jia, L., & Yang, J. (2016). Characterization of O-Carboxymethyl
762 Chitosan – Gum Arabic Coacervates as a Function of Degree of Substitution. *Journal*
763 *of Dispersion Science and Technology*, *37*(9), 1368–1374.
764 https://doi.org/10.1080/01932691.2015.1101609

765 Jayme, M. L., Dunstan, D. E., & Gee, M. L. (1999). Zeta potentials of gum arabic stabilised oil
766 in water emulsions. *Food Hydrocolloids*, *13*(6), 459–465.
767 https://doi.org/10.1016/S0268-005X(99)00029-6

768 Jia, T. Z., Hentrich, C., & Szostak, J. W. (2014). Rapid RNA Exchange in Aqueous Two-Phase
769 System and Coacervate Droplets. *Origins of Life and Evolution of Biospheres*, *44*(1),
770 1–12. https://doi.org/10.1007/s11084-014-9355-8

771 Kaibara, K., Watanabe, T., & Miyakawa, K. (2000). Characterizations of critical processes in
772 liquid–liquid phase separation of the elastomeric protein–water system: Microscopic
773 observations and light scattering measurements. *Biopolymers*, *53*(5), 369–379.
774 https://doi.org/10.1002/(SICI)1097-0282(20000415)53:5<369::AID-BIP2>3.0.CO;2-5

775 Kayitmazer, A. B. (2017). Thermodynamics of complex coacervation. *Advances in Colloid and*
776 *Interface Science*, *239*, 169–177. https://doi.org/10.1016/j.cis.2016.07.006

777 Kizilay, E., Kayitmazer, A. B., & Dubin, P. L. (2011). Complexation and coacervation of
778 polyelectrolytes with oppositely charged colloids. *Advances in Colloid and Interface*
779 *Science*, *167*(1–2), 24–37. https://doi.org/10.1016/j.cis.2011.06.006

780 Kötz, J., Kosmella, S., & Beitz, T. (2001). Self-assembled polyelectrolyte systems. *Progress in*
781 *Polymer Science*, *26*(8), 1199–1232. https://doi.org/10.1016/S0079-6700(01)00016-8

782 Lopez-Torrez, L., Costalat, M., Williams, P., Doco, T., & Sanchez, C. (2015). Acacia senegal
783 vs. Acacia seyal gums – Part 1: Composition and structure of hyperbranched plant
784 exudates. *Food Hydrocolloids*, *51*, 41–53.
785 https://doi.org/10.1016/j.foodhyd.2015.04.019

786 Maqbool, M., Ali, A., & Alderson, P. G. (2010). A combination of gum arabic and chitosan can
787 control anthracnose caused by Colletotrichum musae and enhance the shelf-life of banana fruit.
788 *Journal of Horticultural Science & Biotechnology*, *85*(5), 432–436.
789 https://doi.org/10.1080/14620316.2010.11512693

790 McNamee, B. F., O'Riorda, E. D., & O'Sullivan, M. (1998). Emulsification and
791 Microencapsulation Properties of Gum Arabic. *Journal of Agricultural and Food*
792 *Chemistry*, *46*(11), 4551–4555. https://doi.org/10.1021/jf9803740

793 Meyer, E., Rosenberg, K. J., & Israelachvili, J. (2006). Recent progress in understanding
794 hydrophobic interactions. *Proceedings of the National Academy of Sciences*.
795 https://doi.org/10.1073/pnas.0606422103

796 Moschakis, T., Murray, B. S., & Biliaderis, C. G. (2010). Modifications in stability and
797 structure of whey protein-coated o/w emulsions by interacting chitosan and gum arabic
798 mixed dispersions. *Food Hydrocolloids*, *24*(1), 8–17.
799 https://doi.org/10.1016/j.foodhyd.2009.07.001

800 Mosquera, L. H., Moraga, G., & Martínez-Navarrete, N. (2012). Critical water activity and
801 critical water content of freeze-dried strawberry powder as affected by maltodextrin and
802 arabic gum. *Food Research International*, *47*(2), 201–206.
803 https://doi.org/10.1016/j.foodres.2011.05.019

804 Neel, A. J., Hilton, M. J., Sigman, M. S., & Toste, F. D. (2017). Exploiting non-covalent π
805 interactions for catalyst design. *Nature*, *543*(7647), 637–646.
806 https://doi.org/10.1038/nature21701

807 Padala, S. R., Williams, P. A., & Phillips, G. O. (2009). Adsorption of Gum Arabic, Egg White
808 Protein, and Their Mixtures at the Oil−Water Interface in Limonene Oil-in-Water
809 Emulsions. *Journal of Agricultural and Food Chemistry*, *57*(11), 4964–4973.
810 https://doi.org/10.1021/jf803794n

811 Poudyal, R. R., Guth-Metzler, R. M., Veenis, A. J., Frankel, E. A., Keating, C. D., &
812 Bevilacqua, P. C. (2019). Template-directed RNA polymerization and enhanced
813 ribozyme catalysis inside membraneless compartments formed by coacervates. *Nature*
814 *Communications*, *10*(1), 490. https://doi.org/10.1038/s41467-019-08353-4

815 Priftis, D., Laugel, N., & Tirrell, M. (2012). Thermodynamic Characterization of Polypeptide
816 Complex Coacervation. *Langmuir*, *28*(45), 15947–15957.
817 https://doi.org/10.1021/la302729r

818 Qin, J., & Gronenborn, A. M. (2014). Weak protein complexes: Challenging to study but
819 essential for life. *The FEBS Journal*, 1948–1949. https://doi.org/10.1111/febs.12744

820 Renard, D., Garnier, C., Lapp, A., Schmitt, C., & Sanchez, C. (2012). Structure of
821 arabinogalactan-protein from Acacia gum: From porous ellipsoids to supramolecular
822 architectures. *Carbohydrate Polymers*, *90*(1), 322–332.
823 https://doi.org/10.1016/j.carbpol.2012.05.046

824 Roldan-Cruz, C., Carmona-Ascencio, J., Vernon-Carter, E. J., & Alvarez-Ramirez, J. (2016).
825 Electrical impedance spectroscopy for monitoring the gum Arabic–chitosan
826 complexation process in bulk solution. *Colloids and Surfaces A: Physicochemical and*
827 *Engineering Aspects*, *495*, 125–135. https://doi.org/10.1016/j.colsurfa.2016.02.004

828 Sahoo, J. K., VandenBerg, M. A., & Webber, M. J. (2018). Injectable network biomaterials via
829 molecular or colloidal self-assembly. *Advanced Drug Delivery Reviews*, *127*, 185–207.
830 https://doi.org/10.1016/j.addr.2017.11.005

831 Sakloetsakun, D., Preechagoon, D., Bernkop-Schnürch, A., & Pongjanyakul, T. (2015).
832 Chitosan–gum arabic polyelectrolyte complex films: physicochemical, mechanical and
833 mucoadhesive properties. *Pharmaceutical Development and Technology*, 1–10.
834 https://doi.org/10.3109/10837450.2015.1035727

835 Schatz, C., Lucas, J.-M., Viton, C., Domard, A., Pichot, C., & Delair, T. (2004). Formation and
836 Properties of Positively Charged Colloids Based on Polyelectrolyte Complexes of
837 Biopolymers. *Langmuir*, *20*(18), 7766–7778. https://doi.org/10.1021/la049460m

838 Soni, B., Mahmoud, B., Chang, S., El-Giar, E. M., & Hassan, E. B. (2018). Physicochemical,
839 antimicrobial and antioxidant properties of chitosan/TEMPO biocomposite packaging

films. *Food Packaging and Shelf Life*, *17*, 73–79. https://doi.org/10.1016/j.fpsl.2018.06.001

Sonia, T. A., & Sharma, C. P. (2012). An overview of natural polymers for oral insulin delivery. *Drug Discovery Today*, *17*(13–14), 784–792. https://doi.org/10.1016/j.drudis.2012.03.019

Tan, C., Xie, J., Zhang, X., Cai, J., & Xia, S. (2016). Polysaccharide-based nanoparticles by chitosan and gum arabic polyelectrolyte complexation as carriers for curcumin. *Food Hydrocolloids*, *57*, 236–245. https://doi.org/10.1016/j.foodhyd.2016.01.021

Turgeon, S. L., Schmitt, C., & Sanchez, C. (2007). Protein–polysaccharide complexes and coacervates. *Current Opinion in Colloid & Interface Science*, *12*(4–5), 166–178. https://doi.org/10.1016/j.cocis.2007.07.007

Verbeken, D., Dierckx, S., & Dewettinck, K. (2003). Exudate gums: Occurrence, production, and applications. *Applied Microbiology and Biotechnology*, *63*(1), 10–21. https://doi.org/10.1007/s00253-003-1354-z

Vuillemin, M. E., Michaux, F., Adam, A. A., Linder, M., Muniglia, L., & Jasniewski, J. (2020). Physicochemical characterizations of gum Arabic modified with oxidation products of ferulic acid. *Food Hydrocolloids*, *107*, 105919. https://doi.org/10.1016/j.foodhyd.2020.105919

Vuillemin, M. E., Michaux, F., Muniglia, L., Linder, M., & Jasniewski, J. (2019). Gum Arabic and chitosan self-assembly: Thermodynamic and mechanism aspects. *Food Hydrocolloids*, *96*, 463–474. https://doi.org/10.1016/j.foodhyd.2019.05.048

Vuillemin, M. E., Muniglia, L., Linder, M., Bouguet-Bonnet, S., Poinsignon, S., Dos Santos Morais, R., Simard, B., Paris, C., Michaux, F., & Jasniewski, J. (2021). Polymer functionalization through an enzymatic process: Intermediate products characterization and their grafting onto gum Arabic. *International Journal of Biological Macromolecules*, *169*, 480–491. https://doi.org/10.1016/j.ijbiomac.2020.12.113

Weinbreck, Nieuwenhuijse, H., Robijn, G. W., & de Kruif, C. G. (2004). Complexation of Whey Proteins with Carrageenan. *Journal of Agricultural and Food Chemistry*, *52*(11), 3550–3555. https://doi.org/10.1021/jf034969t

Whitesides, G. M., Mathias, J. P., & Seto, C. T. (1991). Molecular self-assembly and nanochemistry: A chemical strategy for the synthesis of nanostructures. *Science*, *254*(5036), 1312–1319. https://doi.org/10.1126/science.1962191

Yewdall, D. N. A., Buddingh, B. C., Altenburg, W. J., Timmermans, S. B. P. E., Vervoort, D. F. M., Abdelmohsen, P. L. K. E. A., Mason, D. A. F., & Hest, P. J. C. M. van. (2019). Physicochemical Characterization of Polymer- Stabilized Coacervate Protocells. *Chembiochem*, *20*(20), 2643. https://doi.org/10.1002/cbic.201900195

Ziegler, A., & Seelig, J. (2004). Interaction of the Protein Transduction Domain of HIV-1 TAT with Heparan Sulfate: Binding Mechanism and Thermodynamic Parameters. *Biophysical Journal*, *86*(1), 254–263. https://doi.org/10.1016/S0006-3495(04)74101-6

Table captions

Table 1: Approximate Zeta potential of native chitosan (NCN, 0.02% w/v), functionalized chitosan (FCN, 0.02% w/v), native gum Arabic (NGA, 0.50% w/v) and functionalized gum Arabic (FGA, 0.50% w/v) solutions in acetic acid 1.00% v/v at pH 5.5, 45 °C. "a, b, and c" mean that the statistical analysis showed no significant differences between the results.

Table 2: Thermodynamic parameters (dissociation constant (Kd), stoichiometry (n), enthalpic contribution (ΔH), thermo-entropic contribution (TΔS) and Gibbs free energy (ΔG)) of binding between native gum Arabic (NGA)/functionalized gum Arabic (FGA) and native chitosan (NCN)/functionalized chitosan (FCN). "a, b and c" mean that the statistical analysis showed no significant differences between the results, for each column. Results with the same letter means there was no significant difference between them.

Table 1:

Approximate Zeta Potential (mV)			
NCN 0.02% w/v in acetic acid	FCN 0.02% w/v in acetic acid	NGA 0.50% w/v in acetic acid	FGA 0.50% w/v in acetic acid
17.4 ± 0.7^{a}	18.1 ± 0.2^{a}	-9.7 ± 0.7^{b}	-21.7 ± 1.1^{c}

Table 2:

Mixtures	Kd.10^{-08}	n	ΔH (kJ.mol^{-1})	TΔS (kJ.mol^{-1})	ΔG (kJ.mol^{-1})
NGA NCN	14.5 ± 0.6^{a}	2.7 ± 0.2^{a}	-965.2 ± 40.7^{a}	-923.6 ± 40.9^{a}	-41.6 ± 0.2^{a}
NGA FCN	13.6 ± 5.3^{a}	3.1 ± 0.2^{ab}	-916.3 ± 48.8^{a}	-874.3 ± 47.7^{a}	-42.0 ± 1.1^{a}
FGA NCN	17.7 ± 6.9^{a}	3.4 ± 0.3^{b}	-913.3 ± 14.7^{a}	-872.2 ± 13.7^{a}	-41.1 ± 1.0^{a}
FGA FCN	0.4 ± 0.2^{b}	6.3 ± 0.6^{c}	-1331.5 ± 23.3^{b}	-1280.4 ± 24.5^{b}	-51.1 ± 1.2^{b}

Figure captions

Figure 1: (A) Corrected heat rate upon time of mixtures between native gum Arabic (NGA) or functionalized gum Arabic (FGA) and native chitosan (NCN) or functionalized chitosan (FCN) at pH 5.5 at 45 °C. (B) Enthalpy and fit upon gum Arabic/chitosan molar ratio of mixtures between native gum Arabic or functionalized gum Arabic and native chitosan or functionalized chitosan at pH 5.5 at 45 °C. Grey points recorded at the beginning of the titration were excluded from the fit.

Figure 2: (A) Approximate Zeta potential (mV) and (B) turbidity (cm^{-1}), of mixtures between native gum Arabic (NGA) or functionalized gum Arabic (FGA) and native chitosan (NCN) or functionalized chitosan (FCN) upon gum Arabic/chitosan molar ratio at pH 5.5 and 45 °C, 5 min after mixing.

Figure 3: Macroscopic observations of mixtures between native gum Arabic (NGA) or functionalized gum Arabic (FGA) and native chitosan (NCN) or functionalized chitosan (FCN) mixtures upon molar ratio at 45 °C, 5 min after mixing.

Figure 4: Optical micrographs of mixture between native gum Arabic (NGA) or functionalized gum Arabic (FGA) and native chitosan (NCN) or functionalized chitosan (FCN) mixtures upon different GA/CN molar ratios 5 min after mixing at 45 °C, pH 5.5.

Figure 5: Schematic representation of the possible interactions between native gum Arabic (NGA) or functionalized gum Arabic (FGA) and native chitosan (NCN) or functionalized chitosan (FCN).

Figure 1:

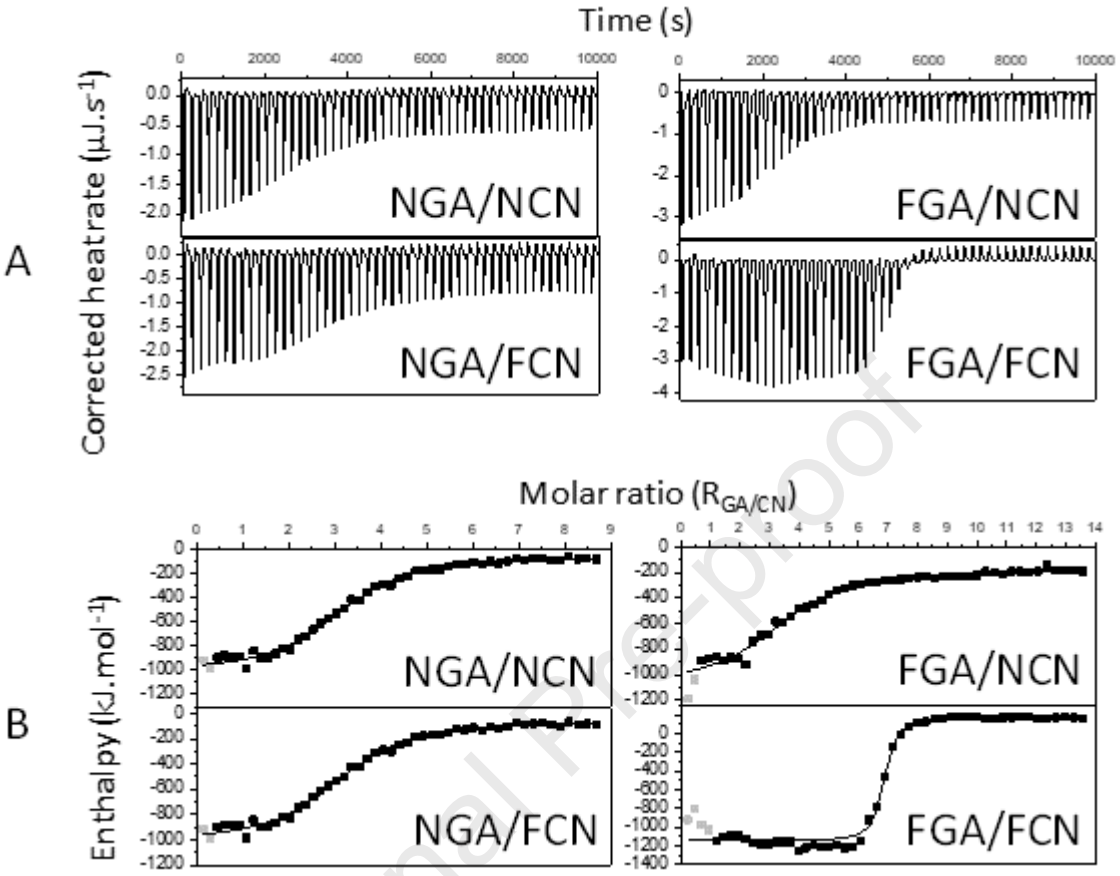

Figure 2:

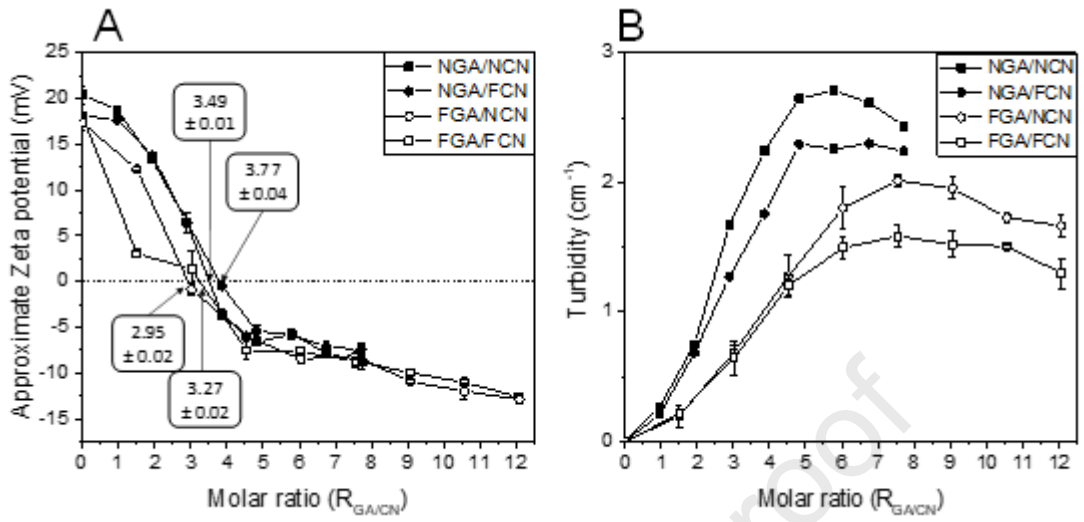

Figure 3:

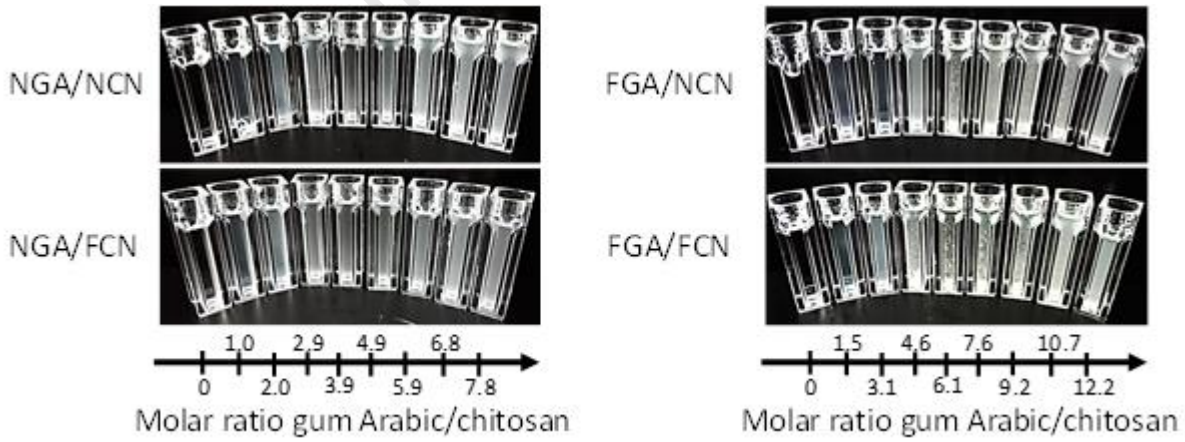

Figure 4:

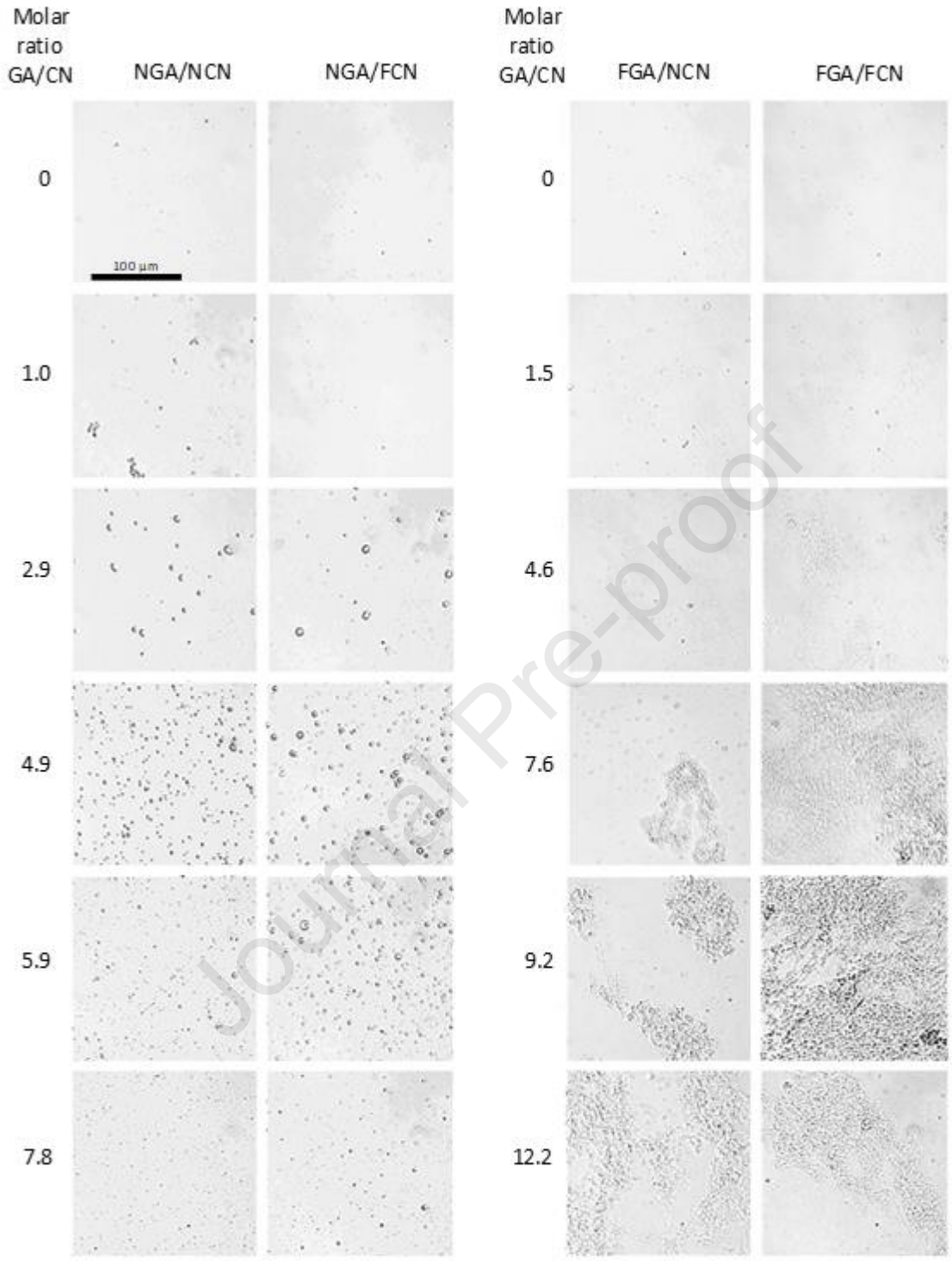

Figure 5:

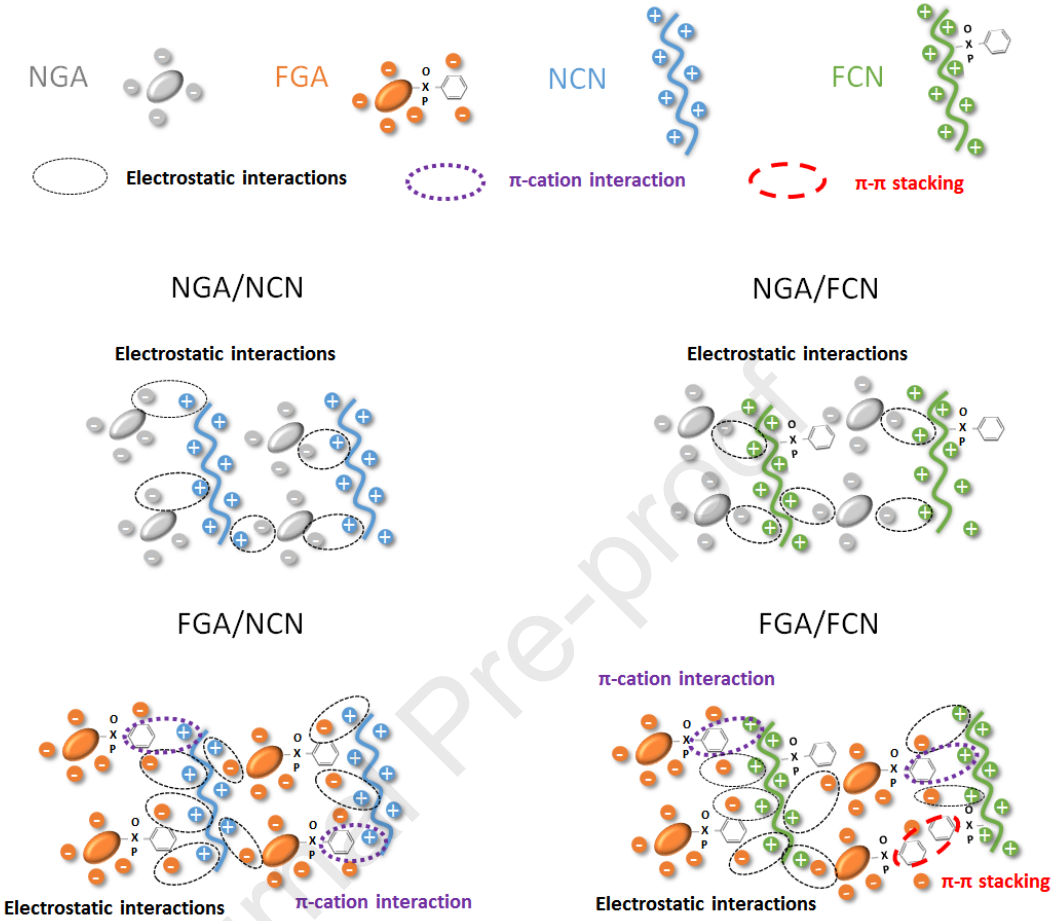

Highlights:

- Grafting phenolic compounds onto polymers changed interactions and objects.
- Polymer functionalization increased their ability to exhibit π interactions.
- New interactions type, led to the formation of different objects.
- In some conditions, coacervates and aggregates coexisted.

Declaration of interests

The authors declare that they have no known competing financial interests or personal relationships that could have appeared to influence the work reported in this paper.